ISAS - INTERNATIONAL SCHOOL FOR ADVANCED STUDIES

Glycine activated whole-cell and single-channel currents in rat cerebellar granule cells in culture

Thesis submitted for the degree of *Doctor Philosophiæ*

CANDIDATE

Caterina Virginio

SUPERVISOR

Prof. Enrico Cherubini

December 1995

SISSA - SCUOLA INTERNAZIONALE SUPERIORE DI STUDI AVANZATI

TRIESTE

Strada Costiera 11

TRIESTE

Glycine activated whole-cell and single-channel currents in rat cerebellar granule cells in culture

Thesis submitted for the degree of *Doctor Philosophiæ*

CANDIDATE

Caterina Virginio

SUPERVISOR

Prof. Enrico Cherubini

December 1995

Notes

During the accomplishment of this thesis, the following papers and posters have been published and presented:

1. Moran O, Zegarra-Moran O, Virginio C and Rottini GD (1991) Voltage dependent cationic channel formed by a cytolytic toxin. *FEBS Lett* 283:317-320.
2. Moran O, Zegarra-Moran O, Virginio C, Gusmani L and Rottini GD (1992) Physica characterization of the pore forming cytolysine from *Gardnerella vaginalis*. *FEMS Lett* 105:63-70.
3. Nizzari M, Sesti F, Giraudo MT, Virginio C, Cattaneo A and Torre V (1993) Single-channel propertiess of cloned cGMP-acivated channels from retinal rods. *Proc R Soc Lond* 254:69-74.
4. Virginio C and Cherubini E (1995) Functional expression of voltage-dependent sodium channels in *Xenpus* oocytes injected with mRNA from neonatal or adult rat brain. *Dev Brain Res* 87:153-159.
5. Virginio C, Martina M and Cherubini E (1995) Spontaneous GABA-mediated synaptic currents in cerebellar granule cells in culture. *NeuroReport* 6:1285-1289.
6. Moran O, Ballarin C, Sorgato MC and Cherubini E (1992) Cationic chahnnels in brain synaptosomal membranes. Annual meeting of the Biophysical Society, Houston.
7. Virginio C and Cherubini E (1994) Functional expression of voltage-dependent sodium channels in *Xenopus* oocytes injected with mRNA from neonatal or adult rat brain. Annual meeting of the American Society for Neuroscience, Miami Beach.

Contents

Chapter 1

Introduction

1.1 Ligand-gated ion channels: the receptor superfamily

Ionic channels are macromolecular pores adapted to the role of regulating the transmembrane flow of ions. Two distinct groups of ionic channels can be recognized on the basis of the stimulus needed to gate them: the voltage gated and the ligand gated channels. The sequencing of genes that encode for ionic channels allow us to reveal strong structural similarities among groups of channels. Now we can talk about families of homologous channel proteins that would have evolved from duplications and divergences of an ancestral gene. Inside this family, the superfamily of receptor channel proteins with similar structural features and evolutionary conserved motifs is present (Hille, 1992).

Signal transmission at chemical synapses involves the receptor channels superfamily that transduce neurotransmitter binding into electrical signals. These ligand-gated ion channels mediate rapid transduction events (less than one millisecond). $GABA_A$, glycine, muscle and neuronal nicotinic acetylcholine, N-methyl-D-aspartate, kainate, AMPA and serotonin ($5\text{-}HT_3$) belong to this class (Hille, 1992; Barnard, 1992; Betz, 1990). The ATP (P_{2X}) receptor is also a ligand gated channel but its structural motif is different from that of channels of this superfamily (Valera et al, 1994; Brake et al, 1994; Surprenant et al, 1995).

Ligand-gated ionic channels for amino acid transmitters have been isolated, and their cDNA have been cloned and sequenced. Hydropathy analysis predicts a cleavable signal sequence, an extended hydrophilic extracellular domain with

potential glycosylation sites and in the C-terminal half, four hydrophobic segments (M1-M4) of sufficient length to form transmembrane α-helices for the subunits of each of these receptors. (Figure 1.1). Each channel is a multisubunit glycoprotein in which the subunits are arranged in a pseudo-symmetric fashion, thus forming a central aqueous pore (Unwin, 1993).

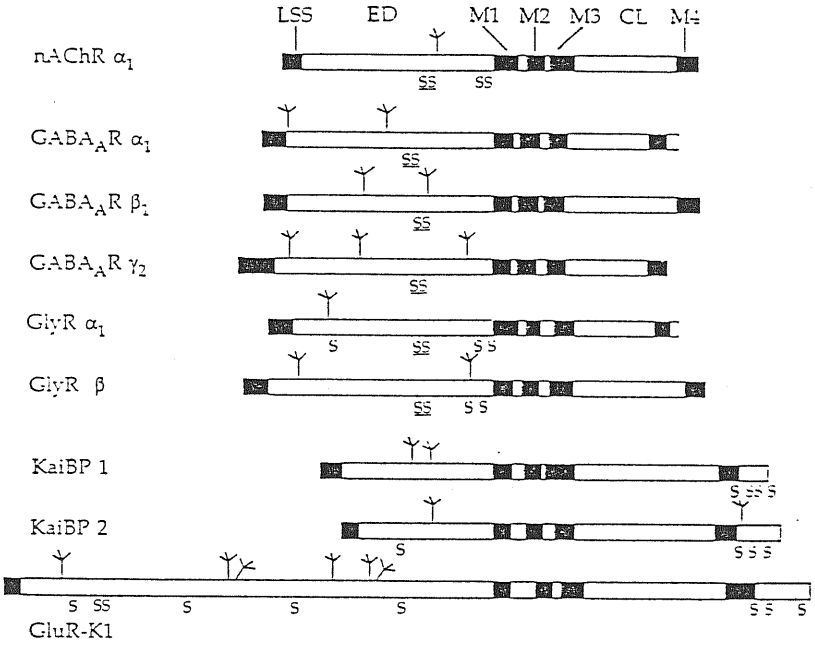

Figure 1.1 Structure of various aminoacid receptor proteins. The putative signal peptide (LSS) and the transmembrane segments (M1-M4) are indicate by black bars, exposed hydrophilic regions by open bars, cysteine residues by S, the conserved cysteine domains by SS and potential N-glycosylation sites by branch structures. All polypeptides are assumed to display the transmembrane topology of nAChR subunits, i.e., having both N-and C-termini located extracellularly. Note variable length of the extracellular domains (ED) and cytoplasmic loop regions (CL). (From Betz,1990).

Another class of molecules are the receptors coupled to a second messanger or to a G protein for their transduction, with the channel involved being separated from the receptor. These kind of receptors operate on a slower time scale (in the millisecond to second range). Muscarinic acetylcholine, quisqualate, $GABA_B$, serotonin (5-HT_1 and 5-HT_2), ATP (P_{2Y} and P_{2U}), histamine (H_1, H_2 and H_3), catecholamines, peptides, light, odorants and tastants receptors belong to this category (Hille, 1992).

1.2 Glycine receptors

Glycine is considered to be the major inhibitory neurotransmitter in the spinal cord and brain stem, whereas γ-aminobutyric acid (GABA) is the major inhibitory neurotransmitter in higher regions of the central nervous system (Kelly and Krnjevic, 1968; Curtis and Johnston, 1974). Glycine and GABA are small amino acid molecules as shown in Figure 1.2. Both inhibit neuronal firing and stabilize the resting membrane potential by binding to pharmacologically distinct receptors, which increase the chloride permeability of the neuronal membrane and thus antagonize the depolarization by Na^+ influx. Glycinergic inhibition is selectively antagonized by the convulsive plant alkaloid strychnine (Curtis et al, 1968) whereas $GABA_A$-mediated inhibitory responses are competitively blocked by bicuculline and allosterically modulated by several compounds, some of them of therapeutic interest such as barbiturates and benzodiazepines (Olsen, 1982). Two decades ago, a postsynaptic receptor protein specific for glycine, the glycine receptor (GlyR), was identified by ligand binding studies (Young and Snyder, 1973; 1974) and was shown to be different from the GABA receptor (Sigel and Barnard, 1984). The GlyR can be activated also by other amino acids

which differ from glycine (for the length of the carbon chain or for the presence of hydroxidic groups or for a cyclic structure as shown in Figure 1.2). In spinal cord neurons, the potency at eliciting inhibition decreases in the following order: glycine > β-alanine > taurine >> L-alanine, L-serine > proline (Langosch et al, 1990; Becker, 1992). GlyR was purified from the mammalian central nervous system and its subunits composition and sequences were determined (Langosch et al, 1990). In the following paragraphs the structure, the molecular heterogeneity and the localization of glycine receptors will be discussed.

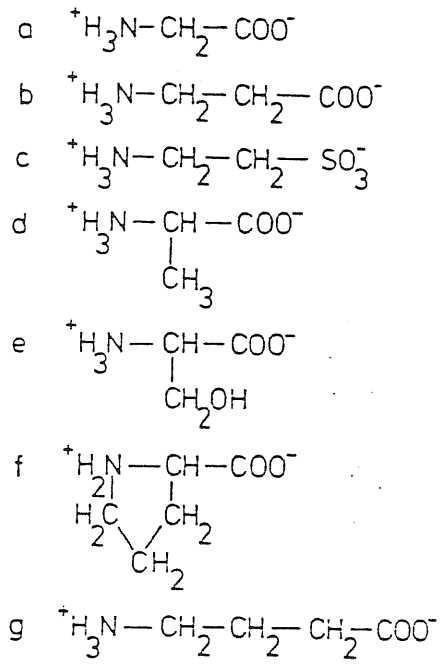

Figure 1.2 Structure of GlyR agonists. (a) Glycine, (b) β-alanine, (c) taurine, (d) alanine, (e) serine, (f) proline and (g) GABA. (From Betz, 1987).

1.2.1 Structure

The inhibitory GlyR was isolated from detergent extracts of rat spinal cord membranes using a strychnine affinity matrix (Pfeiffer et al, 1982). SDS-Polyacrylamide gel electrophoresis of affinity purified GlyR preparations revealed three major polypeptide species: two glycosylated and one non glycosilated protein bands. The glycosylated protein bands with molecular masses of 48 and 58 kDa represent integral membrane-spanning subunits of the receptor (α and β subunits respectively), which, upon solubilization, sediment as a macromolecular complex of 250 kDa. Photoaffinity labelling experiments using [^{3}H]strychnine have localized the ligand binding site of the GlyR to the α subunit (Graham et al, 1983). The non glycosylated protein of 93 kDa copurified with the α and β subunits (Schmitt et al, 1987; Becker et al, 1989) is associated with the cytoplasmic face of the glycinergic postsynaptic membrane (Triller et al, 1985). The presence of this protein at that location and its capacity to bind to polymerized tubulin (Kirsch et al, 1991) are consistent with an anchoring function to imobilize the GlyR complex to the postsynaptic membrane. For this reason the 93 kDa protein has been called gephyrin (from the greek γεφνρα = "bridge"). Infact gephyrin is essential for the formation of glycine receptor clusters (Kirsch et al, 1993b) and it is widely expressed in the central nervous system (Kirsch et al, 1993a). The basic functional properties of the GlyR are preserved during purification. In fact α and β subunits reconstituted in lipid vesicles display chloride flux upon application of glycine or glycine agonists. This agonist-induced chloride flux is blocked by strychnine (Garcia-Calvo, 1989).

Either the ligand-binding α or the presumptive "structural" β subunit alone, when expressed in oocytes (Grenningloh et al, 1990b; Schmieden et al, 1989; 1992;

Kuhse et al, 1990a; 1990b) or mammalian cells (Sontheimer et al, 1989; Bormann et al, 1993) produce glycine-activated chloride currents. The β-homo-oligomer which responds only weakly to glycine, with a Hill coefficient of 1, is strychnine insensitive and is only poorly inhibited by picrotoxin, usually used as a putative $GABA_A$ receptor chloride channel blocker. In contrast, the α-homo-oligomer is highly strychnine-sensitive, has an EC_{50} for glycine 100 times lower than that of the β subunit and has a Hill coefficient of 3. Coexpression of α and β subunits results in hetero-oligomeric channels that in comparison to α-homo-oligomeric channels are 50- to 200-fold less sensitive to picrotoxin block (Pribilla et al, 1992).

Cross-linking, sedimentation analysis of the affinity-purified GlyR and its reaction with anti-α and anti-β subunit antibodies, indicate that the receptor subunits form a pentamer, with a putative α:β stoichiometry of 3:2 (Langosch et al, 1988). The pentameric structure is conserved in other members of the ligand-gated ion channel superfamily, e.g., the nicotinic acetylcholine receptor and the GABA receptor.

The primary structure of GlyR α and β subunits have been determined by cDNA sequencing (Grenningloh et al, 1987a;1990). Analysis of the deduced polypeptides uncovered several features wich are shared by other ligand-gated ion channel proteins (Noda et al, 1983; Schofield et al, 1987).

The domains for channel function and ligand binding are as follows.

(i) A cleavable signal sequence at the N-terminus.

(ii) Four hydrophobic segments (M1-M4) long enough to span the hydrophobic core of a lipid bilayer as α-helices. M1-M3 transmembrane segments have a high degree of conservation between GlyR and $GABA_AR$ subunits, suggesting

that these segments are important in chloride channel formation (Grenningloh et al, 1987b). Segment M2 displays a high content of uncharged polar amino acid residues and therefore is thought to provide the hydrophilic inner lining of the chloride channel. Consistent with the hypothesis that the segment M2 provides the aqueous channel interaction site for ions, in comparison to anion channels, the segment M2 of cation channels has more negative charges (Barnard et al, 1987). A pentameric arrangment of segment M2 α-helices of 5 subunits may create a central pore of 0.58 nm in diameter, a value which closely matches the experimentally determined sizes of both GlyR and $GABA_AR$ channels (Bormann et al, 1987). With exception of the GlyR β subunit, the M2 segments of anion-selective GlyR and $GABA_AR$ proteins terminate with positively charged residues both intra- and extra-cellularly. Furthermore, positively charged residues are abundant in close vicinity to the M1 and M3 sequences. These clustered charges in the putative chloride channel-mouth domain, have been implicated in anion binding and channel selectivity (Grenningloh et al, 1987a; Schofield et al, 1987). Patch-clamp data indicate two sequentially occupied anion binding sites (Bormann et al, 1987). Cation conducting nicotinic acetylcholine receptors, in contrast, have negatively charged side chains in addition to positive charges bordering transmembrane segment M2 (Noda et al, 1983; Numa, 1989). Indeed, the rings of negatively charged residues bordering the M2 regions of this receptor have been shown to determine the conductivity of this cation channel (Imoto et al, 1988).

(iii) The extended N-terminal extracellular domain contains a pair of cysteine residues, whose positions are conserved between different subunits of amino acid gated ion channels (Figure 1.1). For the nicotinic acetylcholine receptor,

these cysteines have been proposed to form a disulfide bridge essential for receptor tertiary structure and/or subunit assembly (Mishina et al, 1985). Thus, also for GlyR, a similar role of these residues may be assigned and a similar folding pattern may exist. The mechanism of agonist discrimination at these receptors is not undertstood. Covalent labeling and site-directed mutagenesis experiments indicate that several discontinuous domains in the N-terminal extracellular region contribute to the formation of the binding pocket (Graham et al, 1983; Schmieden et al, 1992; 1993). Evidence that multiple side-chain in the second half of the extracellular domain of α subunits are involved in the formation of the ligand-binding site of the GlyR also comes from analysis of agonist responses (Horikoshi et al 1988; Schmieden et al, 1989). Comparison of agonist efficacy profiles of expressed α1 and α2 subunit receptor combined with substitution of several divergent amino acids by oligonucleotide-directed mutagenesis revealed two positions, isoleucine 111 and alanine 212 of the α1 subunit, as major determinants of β-alanine and taurine activation sites (Schmieden et al, 1992). These data have led to a multi-site model of the GlyR's ligand-binding region, which includes both high- and low-affinity agonist subsites within an extended binding domain encompassing a major portion of the extracellular region of α subunits (Schmieden et al, 1992). Accordingly, ligand recognition implies interactions with several side-chains folding together in the assembled GlyR channel complex. Within the N-terminal region, in accordance with the glycoprotein nature of these proteins, potential N-glycosylation sites are present.

(iv) A large intracellular hydrophilic loop between segments M3 and M4, contains consensus sequences for phosphorylation by protein kinase C (PKC).

Therefore it constitutes a potential substrate for protein phosphorylation suggesting a role for PKC in the modulation of GlyR function (Ruiz-Gómez et al, 1991; Vaello et al, 1992; 1994; Schönrock and Bormann, 1995).

A tentative model of the GlyR deduced from these data is presented in Figure 1.3 (Betz, 1992).

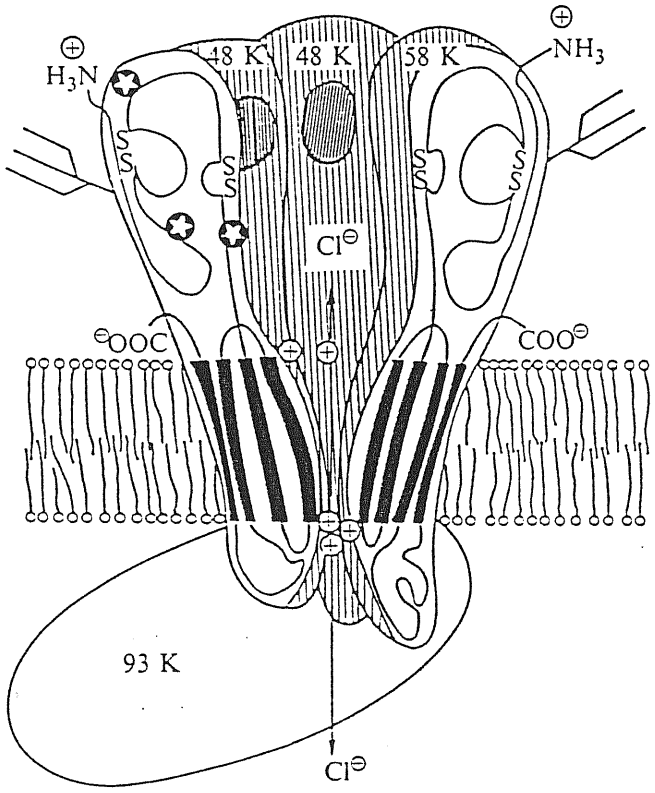

Figure 1.3 The postsynaptic GlyR is shown in a hemisection depicting three of its five membrane spanning subunits. Within the transmembrane portions of the 48 kDa and 58 kDa subunits, the putative transmembrane topologies of the polypeptide chains are depicted. S-S symbolize disulfide bridges, and branched structures putative glycosylation sites. Amino acid positions important for ligand binding as identified by site directed mutagenesis are indicated by asterisk, and positive charges thought to provide chloride binding sites at the inner and outer mouths of the channel by a + sign. Moreover, the position of the cytoplasmatic associated 93 kDa protein gephyrin is outlined. (From Betz, 1992).

1.2.2 Glycine receptor α-subunit variants

Molecular cloning studies have recently revealed that the heterogeneity of GlyRs observed at both the protein and mRNA expression level reflects the existence of several GlyR α-subunit genes. By low stringency screening of cDNA and genomic libraries, clones encoding different isoforms of the originally described GlyR α subunit have been isolated (Langosch et al, 1990). Two variant of the rat α1 cDNAs have been identified (Malosio et al, 1991). Two different α2 cDNAs (α2 and α2*) and an α3 cDNA have been found to be differentially expressed in rats and humans (Grenningloh et al, 1990; Kuhse et al, 1990a; 1990b; 1991). Genomic sequences encoding a fourth variant, the α4, are available from mice (Matzenbach et al, 1994). All these α-subunit sequences display a high degree of amino acid identity with each other and correspond to GlyR polypeptides, the expression of which is under distinct temporal and regional control (Betz, 1991).

Functional expression in *Xenopus* oocytes has allowed a pharmacological characterization of various GlyR α-subunits. Upon injection, α1, α2 and α3 cDNAs generate glycine-gated chloride channels that are blocked by nanomolar concentrations of strychnine and with distinct glycine binding affinities (Schmieden et al, 1989; 1992; Sontheimer et al, 1989; Grenningloh et al, 1990; Kuhse et al, 1990a; 1990b; 1991; Akagi et al, 1991). However, a rat α2 variant sequence, α2*, assembles into channels that display 30-40-fold lower affinity for the agonist glycine and 500-fold lower sensitivity for the antagonist strychnine. α2* is therefore thought to correspond to the ligand-binding subunit of the strychnine-insensitive GlyR in the neonatal rat spinal cord. Using site-directed mutagenesis, it was shown that a single glycine to glutamate exchange at

position 167 of the α2 polypeptide was enough to cause the different pharmacological properties of the two receptors (Kuhse et al, 1990a). Recently, substitution of the homologous residue glycine 160 and the neighbouring tyrosine 161 as well as the distant positions lysine 200 and tyrosine 202 in the human α1 subunit was shown to profoundly reduce strychnine inhibition (Vandenberg et al, 1992). This finding underlines the importance of minor amino acid substitutions for ligand binding, a conclusion further supported by other characteristic differences in agonist-gating profiles between the expressed α1, α2 and α3 subunits (Grenningloh et al, 1990; Kuhse et al, 1990a; 1990b). The alternative splicing of α1 and α2 mRNAs has been shown to be responsible for the creation of additional diversity of GlyR. For the rat α1 subunit, a variant cDNA has been identified that originates from alternate splice acceptor site selection at an exon encoding the cytoplasmic domain adjacent to transmembrane segment M3 (Malosio et al, 1991). This generates a novel consensus phosphorylation site (insertion of eight additional amino acids) in the intracellular loop domain and thus may allow further receptor regulation. Interestingly, an equivalent eight amino acid insertion has also been found for the γ2 subunit of the $GABA_A$ receptor and has been shown to provide a sequence that, *in vitro*, is efficiently phosphorylated by protein kinase C (Whiting et al, 1990). In the rat α2 gene, alternative use of the two closely spaced versions of exon 3 generates subunit isoforms, which differ by only two isofunctional amino acid substitutions in the N-terminal extracellular region (Kuhse et al, 1991). Whether similar variants generated by alternative splicing also exist for other GlyR α subunit transcripts is presently unclear. However, the

data obtained so far underline the importance of post-transcriptional processing in generating GlyR diversity (Betz ,1991).

1.2.3 Heterogeneity of glycine receptor in the CNS during development

Pharmacological, biochemical and cDNA sequencing data have established subtype diversity as a general phenomenon for receptors in the CNS (Betz, 1990). Evidence for subtype heterogeneity of the GlyR was first detected in studies of rodent spinal cord development, in which a neonatal isoform prevalent at birth was shown to differ from the adult GlyR in pharmacological, immunological and biochemical properties (Becker et al, 1988; Hoch et al, 1989). In particular, this neonatal receptor is characterized by low strychnine binding affinity, altered antigenicity and a ligand binding α subunit differing in molecular weight (49 kDa) from that of the adult receptor (48 kDa). The neonatal α subunit is abundant at birth (70% of the total receptor protein). Within 2-3 weeks after birth, the neonatal glycine receptor in the spinal cord is completely replaced by the adult type receptor, resulting in a strong postnatal increase of high affinity [^{3}H]strychnine binding (Becker et al, 1988). Immunological analysis of GlyR expression in postnatal rat cortex indicate a tight developmental regulation with high levels of immunoreactivity at birth, which transiently increased during the second postnatal week, but subsequently declined to low adult levels. Immunologically, cortical GlyRs resemble the neonatal receptor isoform of spinal cord (Becker et al, 1993).

The developmental heterogeneity of the GlyR comes also from mRNA expression studies in *Xenopus* oocytes. Poly(A)$^+$ RNA was isolated from adult rat cerebral cortex and spinal cord and from newborn spinal cord. All three mRNAs

injected into *Xenopus* oocytes cause expression of glycine-gated chloride channels. If each preparation of mRNA is fractionated by sedimentation on sucrose density gradients, two classes of GlyR mRNAs could be separated, both of which gave raise to functional channels when expressed in oocytes (Akagi and Miledi, 1988). A rapidly sedimenting mRNA species was abundant in the spinal cord of adult rats, whereas fractions from the neonatal spinal cord and adult brain cortex contained mainly the smaller GlyR mRNA. The electrophysiological properties of GlyR from the two classes of mRNAs extracted from newborn spinal cord have been found to be different from those from adult spinal cord (Morales et al, 1994). Moreover, hybrid-arrest experiments employing three synthetic oligodeoxynucleotides complementary to different parts of an RNA encoding a glycine receptor subunit allowed further differentiation of the fractionated mRNA (Akagi et al, 1989).

1.2.4 Distribution of glycine receptor in the CNS

The distribution of GlyR in the CNS has been analysed by [^{3}H]strychnine autoradiography of CNS sections (Zarbin et al, 1981; Frostholm and Rotter, 1985; Probst et al, 1986; Frost et al, 1990). These studies disclosed a marked rostro-caudal gradient of the receptors, with highest levels being found in the brain stem and spinal cord. Immunocytochemistry with monoclonal antibodies raised against affinity-purified rat GlyR (Pfeiffer et al, 1984) allowed a more accurate mapping at both light and electron microscope level. The distribution of α subunit antigen and gephyrin were generally found to match that of [^{3}H]strychnine-binding sites, although no perfect overlap was obtained (Triller et al, 1985; 1987; Altschuler et al, 1986; Van den Pol and Gorcs, 1988). Several higher brain regions, including the olfactory bulb, midbrain and cerebellum, displayed low but significant immunoreactivity. Application of a monoclonal

antibody directed against an epitope conserved in the different GlyR α subunit variants (Schröder et al, 1991) has recently modified this picture: immunoreactive cells have now been identified in many higher brain regions including cortex (Naas et al, 1991). An even more complex picture arises from *in situ* hybridization experiments with subunit sequence-specific oligonucleotides (Malosio et al, 1991). In the adult rat, GlyR α1 subunit mRNA was abundant in spinal cord, but was also seen in brain stem and colliculi, whereas α2 transcripts were found in several brain regions including cerebral cortex and hippocampus. GlyR α3 subunit mRNA was expressed at low levels in cerebellum, olfactory bulb and hippocampus, while high amounts of β subunit transcripts were widely distributed throughout spinal cord and brain. During development, α2 mRNA accumulated already prenatally and decreased after birth, whereas α1 and α3 subunit transcripts appeared only in postnatal brain structures. In the cerebellar cortex, a structure that reaches maturity only very late after birth, transient α2 hybridization signals were seen in the first two weeks of postnatal life.

From the localization of the GlyR α subunit transcripts, GlyRs appear to be particularly important in areas implicated in motor and sensory processing.

1.3 Cerebellum

1.3.1 Cellular organization of the cerebellum

The axons entering the cerebellum from the spinal cord, the vestibular nuclei, the pons and elsewhere give off collaterals to the deep cerebellar nuclei and distribute their branches to the deepest layer of the cerebellar cortex, the *granular layer*, constituted by the granule cells, the only excitatory neurons of the

cerebellum. These extremely small neurons with a high packing density use glutamate as neurotransmitter. In the granular layer the branches of afferent fibers (called mossy fibers because they end in large, somewhat lobulated terminals) make synapses with the short, clawlike dendrites of the granule cells (Figure 1.4). In turn the granule cells send thin, unmyelinated axons to the most superficial layer of the cerebellar cortex, the *molecular layer.* It is a stratum occupied largely by neuronal processes. In the molecular layer each arriving axon bifurcates into a left and right collateral. Each collateral runs parallel to the long axis of the folium (the cerebellar convolution) in which the parent fiber arrived. Such collaterals are called parallel fibers. In the molecular layer dendrites of the Purkinje cells are also present: large inhibitory neurons whose flask-shaped cell bodies are found at intervals of about 100 micrometers in a row at the interface between the granule cell layer and the molecular layer, which constitutes the third layer of the cerebellar cortex: the *Purkinje cell layer.* Each Purkinje cell has one or, more commonly, two or three dendritic trunks that rise in the molecular layer. There they produce an extraordinary tree, all in a single plane perpedicular to the long axis of the folium, and thus to the parallel fibers (Figure 1.4). The tree is notable for a wealth of short, thick dendritic spines (preferential sites of synapses). They are sites at which each Purkinje cell receives excitatory signals from the multitude of parallel fibers that pass through its dendritic plane. The axons of Purkinje cells in turn leave the cerebellar cortex and makes GABAergic inhibitory synapses in the deep cerebellar nuclei which project to other brain structures including red nucleus, ventral nucleus of the thalamus and other places beyond the cerebellum.

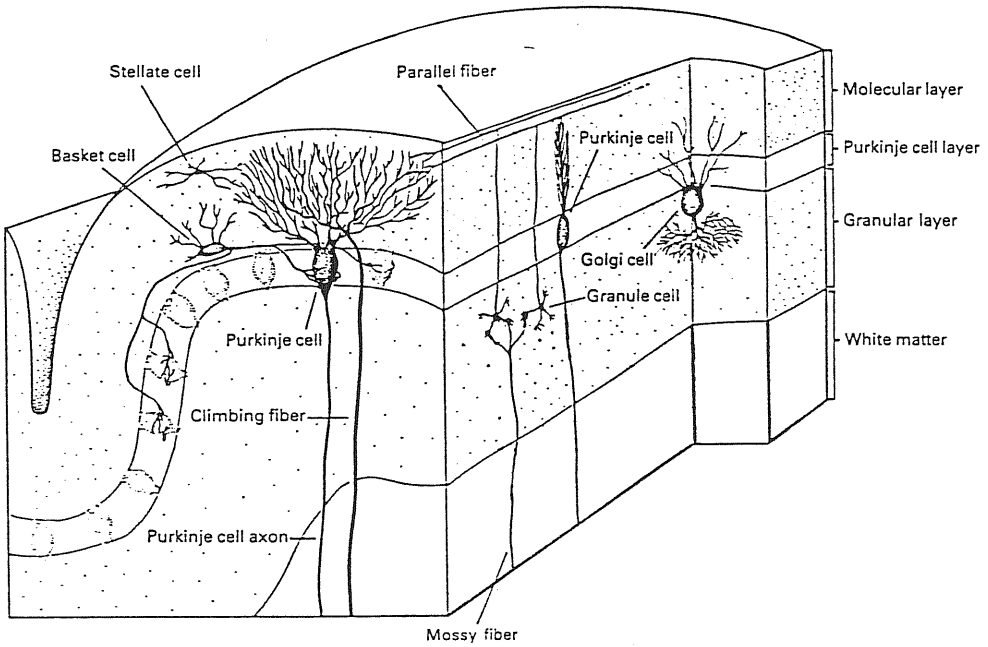

Figure 1.4 Cellular organization of the cerebellum. The cerebellar cortex is organized into three layers and contains five types of neurons. This vertical section of a single cerebellar folium, in both longitudinal and transverse planes, illustrates the general organization of the cerebellar cortex. (From Kandel et al, 1991).

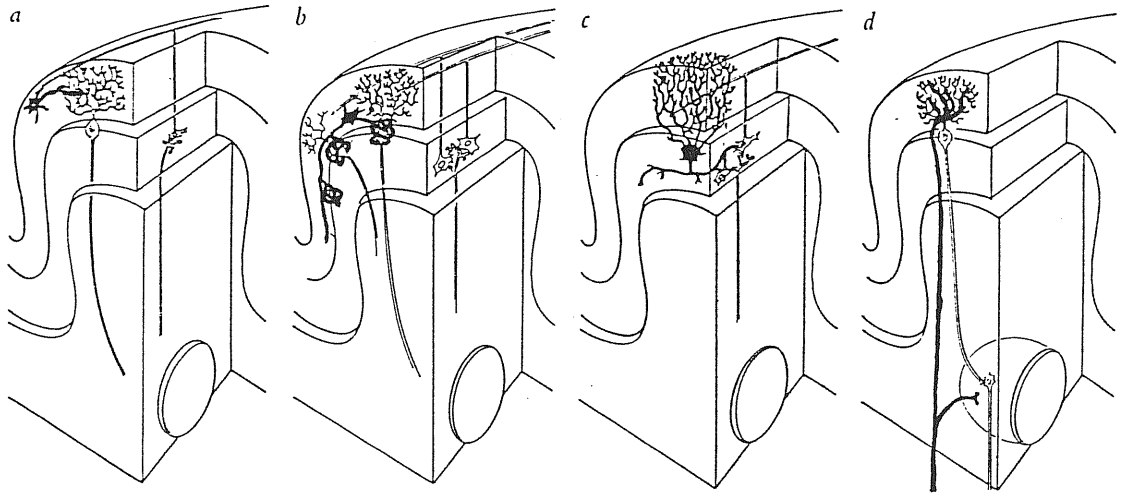

Figure 1.5 Auxiliary circuits of the cerebellum. Two classes of cerebellar neurons, the stellate cells (a) and the basket cells (b) receive their input from parallel fibers and inhibit Purkinje cells. In contrast, the Golgi cells(c) receive the same input but inhibit granule cells. Finally the cererbellar afferents called climbing fibers (d) disinhibit Purkinje cells. (From Nauma and Feirtag, 1986).

There are, however, detours. In particular, the information channeled into the basic pathway from mossy fiber to granule cell to Purkinje cell to deep cerebellar nuclei encounters auxiliary circuits (Figure 1.5). One of them is characterized by stellate cells whose body is in the molecular layer. These cells are so few to give the impression that this layer is devoid of cell bodies. The dendritic tree of stellate cells is flattened into a plane athwart the traffic of parallel fibers. Thus the stellate cell, like the Purkinje cell, gets its input from parallel fibers. Its axon passes above Purkinje cells and makes inhibitory synapses with their dendritic trees.

A second auxiliary circuit in the cerebellar cortex is constituted by the basket cells whose bodies lie deep in the molecular layer. They receive their imputs from parallel fibers and send their axons across folium, over a length of about a millimeter, emitting collaterals that descend to weave axonal baskets around the cell bodies of as many as 12 Purkinje cells. Side branches emerge from the trunk of the axon and also from the collaterals and weave baskets around still other Purkinje cells. In this way a single basket cell participates in weaving axonal baskets around the cell bodies of a hundred or even two hundred Purkinje cells. Conversely, the basket around each Purkinje cell is woven by several basket cells. Their anatomical arrangement suggests that basket cells exert a powerful inhibition on Purkinje cells.

A third circuit is established by Golgi cells whose cell bodies are in the granular layer, just under Purkinje cells. After receiving their imputs from parallel fibers they inhibit granule cells. This inhibition is mediated by GABA (Bisti et al 1971). Golgi cells accumulate and release also the inhibitory neurotransmitter glycine (Morales and Tapia, 1987). Indeed most Golgi cell terminals exhibit both GABA- and glycine-like immunoreactivity (Ottersen et al, 1988; 1990).

In summary, the impulses travelling along parallel fibers are conveyed to the dendrites of four types of cells: Purkinje cells, which are the only projection cells in the circuit, since only their axons leave the cerebellar cortex; basket cells, whose axons exert a powerful inhibition on the cell bodies and initial axon segments of Purkinje cells; stellate cells, whose axons exert a more graded inhibition in the dendritic tree of Purkinje cells; and Golgi cells, whose axons exert an inhibition on granule cells (Figure 1.6).

Finally we have to mention the climbing fibers, the only cerebellar afferents that transmit their influence to Purkinje cells directly. On entering the cerebellum each climbing fiber gives off collaterals to the deep cerebellar nuclei and then it passes straight through the granular layer of the cerebellar cortex, and straight through the Purkinje cell layer as well. In the molecular layer its ramifications cling to the main dendritic trunks of Purkinje cells. Each climbing fiber contacts only 1-10 Purkinje neurons, and each Purkinje cell receives synaptic imput from only a single climbing fiber. The entire extent of the clinging is packed with synatic vesicles. Each climbing fiber tends to be quiescent for some time, and then to give an excitation so intense to erase all preexisting inhibition imposed on that cell by the axons of basket and stellate cells. Climbing fibers originate in the inferior olivary nucleus. They would modify the response of Purkinje cells to mossy fiber inputs for prolonged periods of time (Nauma and Feirtag, 1986; Kandel, 1991).

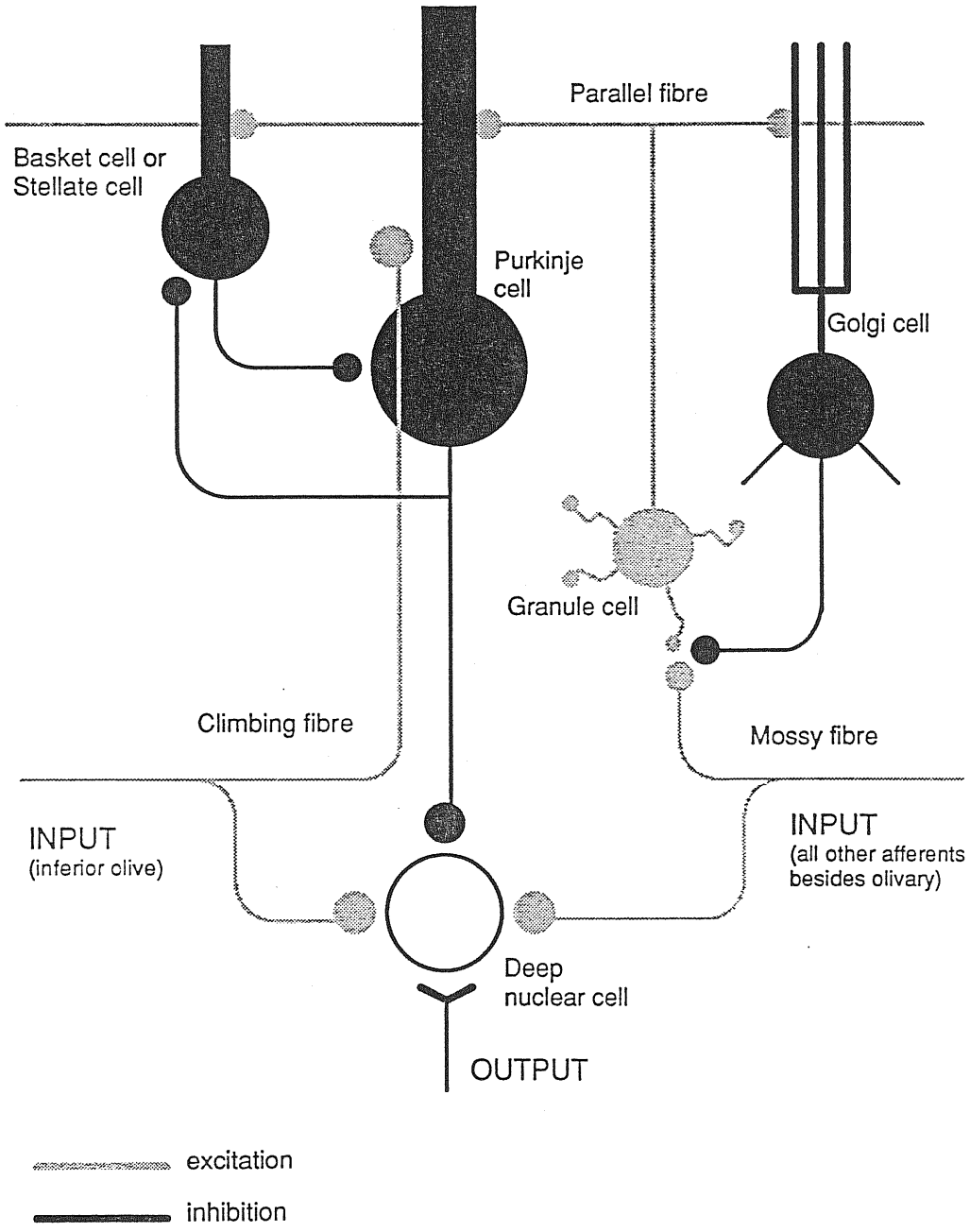

Figure 1.6 Basic neuronal circuit of the cerebellum.

1.3.2 Cerebellar granule cells

As already mentioned, cerebellar granule cells comprise the largest population of identifiable neurons in the vertebrate brain. The granule cells together with the stellate and the basket cells are generated in a displaced proliferative zone, the external germinal layer (Figure 1.7). At early postnatal periods, this layer contains a rapidly dividing population of cells, called neuroblasts, that migrate inwardly between birth and postnatal day 14 to form the internal granular layer (Rakic, 1971). Only Purkinje and Golgi cells are formed in the cerebellar nucleus in embryo. In the late embryonic period the proliferation of immature granule cells depends on homotypic neuron-neuron interactions leading to a rapid thickening of the external germinal layer and restricting the fate of multipotential precursor cells in this proliferative zone to granule neurons. Proliferation continues until interactions with glial cells arrest the divison and subsequently support the migration of terminally differentiated cells into the internal granular layer (Gao et al, 1991).

Granule cells can be isolated and maintained in culture. For this purpose they are prepared from one week old rats, when a large proportion of cells are still immature. Their maturation can be influenced by environmental factors such as high (25 mM) potassium concentration culture medium or excitatory amino acids treatment which mimic the effects of afferent inputs, the glutamatergic mossy fibers (Gallo et al, 1987; Balázs et al, 1988). The high extracellular potassium may induce intracellular events that are normally elicited by the depolarization and activation of voltage-sensitive calcium channels with consequent calcium influx into the cells and induction of an up regulation of N-methyl-D-aspartate receptors (Van der Valk et al, 1991). With an external potassium concentration of 25 mM, the formation of functional synapses is inhibited (Irving et al, 1992);

only small amplitude spontaneous N-methyl-D-aspartate-mediated excitatory synaptic currents can be detected (Kilic et al, 1991). On the other hand, in low (5mM) potassium medium several cells maintain their undifferentiated state and many of them stain positive with antibody for glutamic acid decarboxylase (GAD), the synthetic enzyme for GABA: they therefore synthetize and release GABA as a neurotransmitter (Randall et al, 1993). In fact, in 5 mM potassium, cerebellar granule cells exhibit spontaneous GABA-mediated synaptic currents (Virginio et al, 1995).

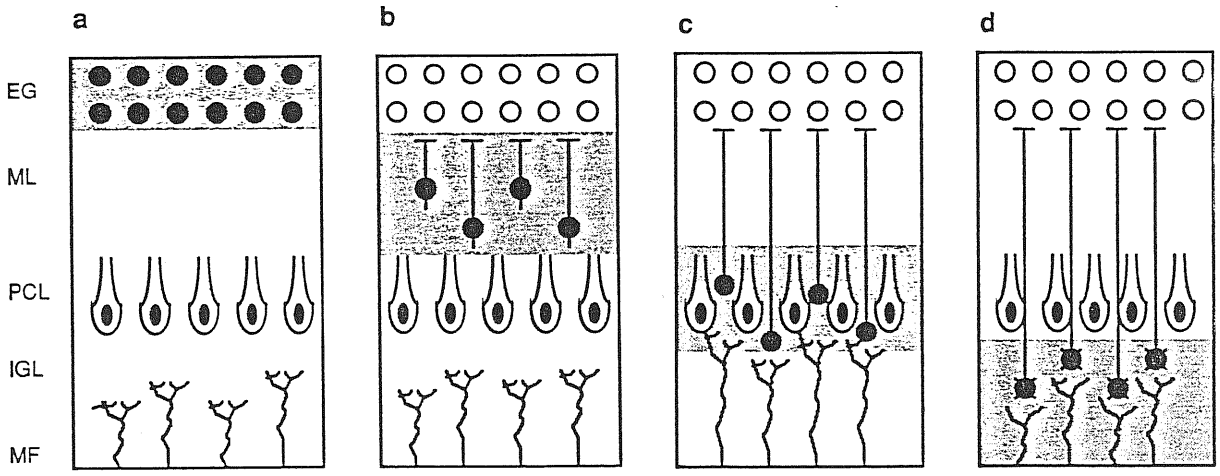

Figure 1.7 Temporal-spatial pattern of differentiation of granule cells in the developing mouse cerebellar cortex. On postnatal day 8, immature granule cells representing each of the major steps in development, neurogenesis, axon outgrowth, migration and synaptogenesis, are distributed in discrete layers of the cerebellar cortex. (a) External germinal layer (EGL) precursor cells undergoing mitosis (filled cells) are located at the pial surface. (b) Postmitotic cells undergoing axon extension and glial guided-migration through the molecular layer (ML) are located below the proliferating precursor cell population. (c) Postmigratory cells are transiting the Purkinje cell layer (PCL) to establish (d) the internal granule cell layer (IGL). The ingrowth of the mossy fibers (MF) is illustrated at the bottom of the panels a-c. (Adapted from Kuhar et al 1993).

Chapter 2

Functional expression of glycine receptors in oocytes injected with neonatal cerebellar mRNA

As already mentioned, in the cerebellar cortex, a structure that reaches maturity only very late after birth, mRNAs for strychnine sensitive GlyR subunits are present only during the first two weeks of postnatal life (Malosio et al, 1991). Moreover functional strychnine sensitive glycine responses have been described in the hippocampus of neonatal animals (Ito and Cherubini, 1991), in hippocampal, cerebellar and cortical cells in culture (Fatima-Shad and Barry, 1992; Huck and Lux, 1987; Siebler et al, 1993) and in *Xenopus* oocytes injected with mRNA isolated from cultured mouse cerebellar granule cells (Wahl et al, 1994). This suggest that inhibitory GlyRs, although not present in higher brain regions of adult animals, may be transiently expressed during development and therefore play a role in early postnatal life.

For this reason in this study, firstly we analyzed whether functional strychnine sensitive GlyRs can be expressed in *Xenopus* oocytes following injection of mRNA isolated from neonatal or adult rat cerebellum (Miledi et al, 1989), and secondly we studied the expression of strychnine sensitive GlyRs in cerebellar granule cells in culture.

2.1 Isolation of rat cerebellum mRNA

Neonatal (< 5 days old) or adult (> 30 days old) Wistar rats were decapitated under ether anaesthesia. The cerebella were dissected free and

immediately frozen in liquid nitrogen. The poly(A)$^+$ mRNA was isolated using the Fast Track mRNA isolation kit (Invitrogen, San Diego, CA, U.S.A.), based on oligo(dT) affinity chromatography. Cerebellar Neonatal or Adult mRNA (NmRNA or AmRNA) was extracted sequentially with equal volumes of phenol, phenol/chloroform, chloroform followed by spectrophotometric quantification of the extracted mRNA, precipitated with Na-acetate and ethanol and stored at -80°C. In the present study four different neonatal and five different adult mRNA preparations were used.

2.2 Expression in oocytes

Ovarian lobes were removed aseptically from adult female Xenopus laevis frogs (NASCO, Ft. Atkinson, WI), anaesthetized by immersion in iced water for 15 to 30 minutes. Stage V or VI oocytes which have a diameter of about one mm were isolated manually in Barth's Solution (BS) containing (in mM): NaCl, 88; KCl, 1; MgSO4, 0.82; Ca(NO3)2, 0.33; CaCl2, 0.41; NaHCO3, 2.4; Tris-HCl, 5 (pH 7.4). Oocytes were defolliculated with collagenase type IA (1 mg/ml, Sigma) and injected with 100 ng of AmRNA or NmRNA reconstituted in a volume of diethylpyrocarbonate-treated water (Sigma) using an automatic injector (Drummond Scientific Co., Broomall, PA). After 3 to 7 days incubation at 19°C in BS containing gentamycin (50 mg/ml, Sigma) and heat inactivated horse serum (5%, Sigma), oocytes were tested for GlyRs expression. Five and seven batches of oocytes extracted from different frogs were used for A or NmRNA respectively.

2.3 Electrophysiological recordings and data analysis

The oocyte was placed in a 300 µl recording chamber and continuously superfused with Normal Frog Ringer of the following composition (in mM): NaCl, 115; KCl, 1.8; CaCl2, 1.8; Hepes, 10 (pH 7.2). Glycine was applied to the oocyte through the perfusion system. Glycine activated currents were recorded at room temperature (20-23°C) with a two-microelectrode voltage-clamp device using a virtual ground circuit. The voltage and current electrodes were filled with filtered 3M K-methyl sulfate and had impedances of 0.5-1 MΩ. Cells with a resting potential more depolarized than -40 mV were discarded.

Data acquisition and analysis were performed using the Acquire and TAC programs of the Instrutech Corporation (Elmont, N.Y.). Data were obtained at the recording frequency of 100 Hz and filtered on line at 1 kHz with an 8-pole Bessel filter before being digitized. Data are expressed as mean ± S.E.M.

2.4 Glycine-activated currents in oocytes

Bath application of glycine (1mM) to oocytes previously injected with neonatal rat cerebellum mRNA, voltage clamped at -80 mV, induced in 14 out of 46 cases, an inward current that slowly reached a peak in few seconds and slowly declined to a plateau level. The mean peak current amplitude was 73.7 ± 22.6 nA (n=14). The effect of glycine was concentration dependent (the maximun response being attained with 5 mM glycine). In two cases a dose response curve was constructed. Data points were fitted with the empirical Hill equation. EC_{50} values were 625 and 730 µM. The amplitude of the current increased with membrane hyperpolarization and decreased with membrane depolarization. In two cases the current became outward at -28.4 and -32.5 mV. These values are very close to the

reversal potential for chloride ions found in oocytes (Barish, 1983) (Figure 2.1). Glycine evoked currents were completely abolished in a reversible manner by 1 μM strychnine, a competitive glycine antagonist (data not shown). In oocytes injected with adult rat cerebellum mRNA glycine (1-5 mM) failed to induce any current (n = 20).

These experiments clearly show that only oocytes injected with mRNA from neonatal rat cerebella are able to express functional strychnine-sensitive glycine receptors.

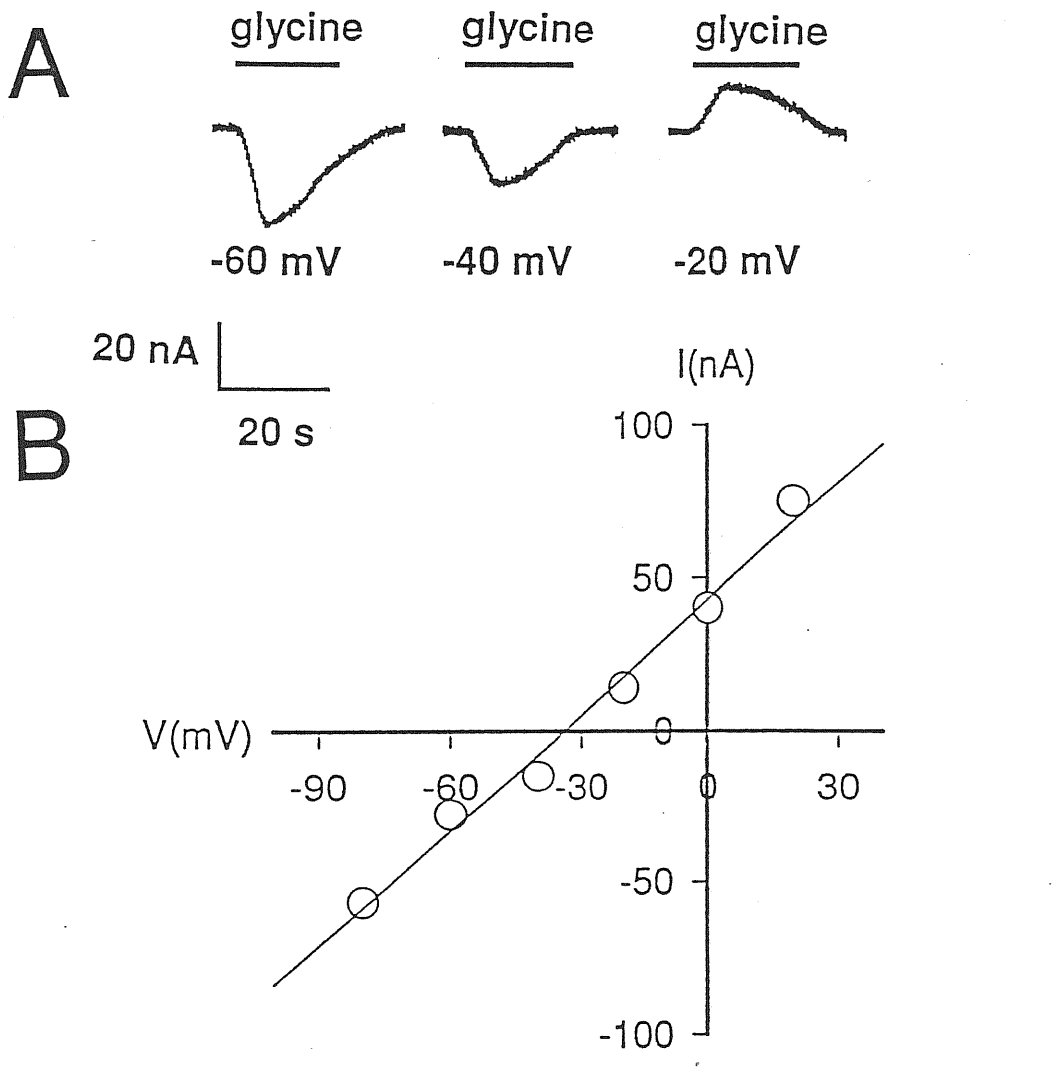

Figure 2.1 Glycine activated currents in an oocyte injected with neonatal rat cerebellar mRNA. (A) Currents evoked by glycine (1 mM, closed bars) at holding potentials indicated below each trace. (B) Peak amplitude of glycine currents are plotted as a function of the holding potential. The I/V relationship was linear in the potential range from -80 to 20 mV. The reversal potential was -33 mV.

Chapter 3

Cerebellar granule cells in culture

Inhibitory GlyRs seem to be transiently expressed during development. *In situ* hybridization experiments for the detection of mRNA for GlyR α subunits in the rat brain have revealed the presence of this nucleic acid in the cerebellum of rats only during the first two postnatal weeks (Malosio et al, 1991). Moreover the expression of GlyRs is detectable only in *Xenopus* oocytes injected with mRNA extracted from neonatal rat cerebellum (present data). Since granule cellls constitute the major neuronal population in the cerebellum, the following experiments have been devoted to see whether these cells express functional GlyRs. In order to maintain granule cells in an undifferentiated state, as they are during the first two weeks of postnatal life, they were grown in a low (5 mM) potassium medium.

3.1 Cell culture preparation

Granule cells were isolated from cerebella of 7 to 9 postnatal day old Wistar rats using a standard procedure (Levi et al, 1984). All steps of preparation were done under sterile conditions. Ether anesthetized rat pups were decapitated and the cerebella were dissected and placed in a solution containing (in mM): NaCl 124, KCl 5.37, NaH_2PO_4 1.01, D-glucose 14.5, Hepes 25, $MgSO_4$ 1.2, phenol red (Sigma) 10 µg/ml, bovine serum albumin (Sigma) 3 mg/ml and gentamicin (Sigma) 100 µg/ml. The cerebella's meninges were carefully peeled off and the cerebella were sliced with a chopper (300 µm thick slices) in one direction and then again at a 90° angle to the previous cuts. The minced tissue was placed in a tube containing the solution

described before, exept gentamicin, and centrifugated at 1000 RPM for 45 s. The cell pellet was treated with 0.25 mg/ml trypsin (Sigma) at 37° for 10 min in order to digest the connective tissue. The action of trypsin was blocked by the addition of 166.4 µg/ml Soybean trypsin inhibitor (Sigma). DNA released from lysed cells was degraded by 25.6 µg/ml DNAse (Sigma). After a rest of 5 min the cells were centrifugated at 1000 RPM for 45 s and placed in the previous described solution exept gentamicin, containing also 240 µg/ml DNAse, 1.56 mg/ml trypsin inhibitor and 5.8 mM $MgSO_4$. Cells were further mechanically dissociated using fire polished Pasteur pipettes of a diameter such as to dissolve cell clumps. Separated cells were washed with a solution containing Ca^{2+}. After a centrifugation at 1000 RPM for 5 min, the pellet of dissociated cells was resuspended in Basal Eagle's medium (Gibco), in which the KCl concentration was 5 mM, supplemented with 2 mM L-glutamine, 20 mM KCl, 100 µg/ml gentamicin and 10% of heat inactivated fetal calf serum (Gibco). Cerebellar granule cells were plated on 35 mm diameter Petri dishes, each containing 2 ml of cell suspension at a density of about $0.5x10^6$ - $1x10^6$ per ml of suspension. Petri dishes had been previously coated with poly L-lysine (Sigma) by incubating for 15 min each dish with 2 ml of poly L-lysine (5 µg/ml). The cells were kept in the incubator (Heraeus B5061 EK-02) at 37° C and 5% CO_2. After one day in culture, the K^+ concentration of the medium was decreased from 25 to 5 mM. To inhibit the growth of non neuronal cells 10 µM of the mitotic inhibitor cytosine β-D-arabino furanoside (Sigma) was added per dish at about 24 hours after plating. In order to provide food for the cells 10 µM D-glucose was added per dish after 7 days in culture (DIC). Under these conditions the cells were maintained in culture for about 15 days and were available for experiments starting from the second day in culture.

Granule cells were >90% of the cells in the culture and were morphologically identified by the oval or round cell body, small size (5-10 μm diameter) and bipolar neurites (Thangnipon et al, 1983). An example of cerebellar granule cell culture is shown in Figure 3.1.

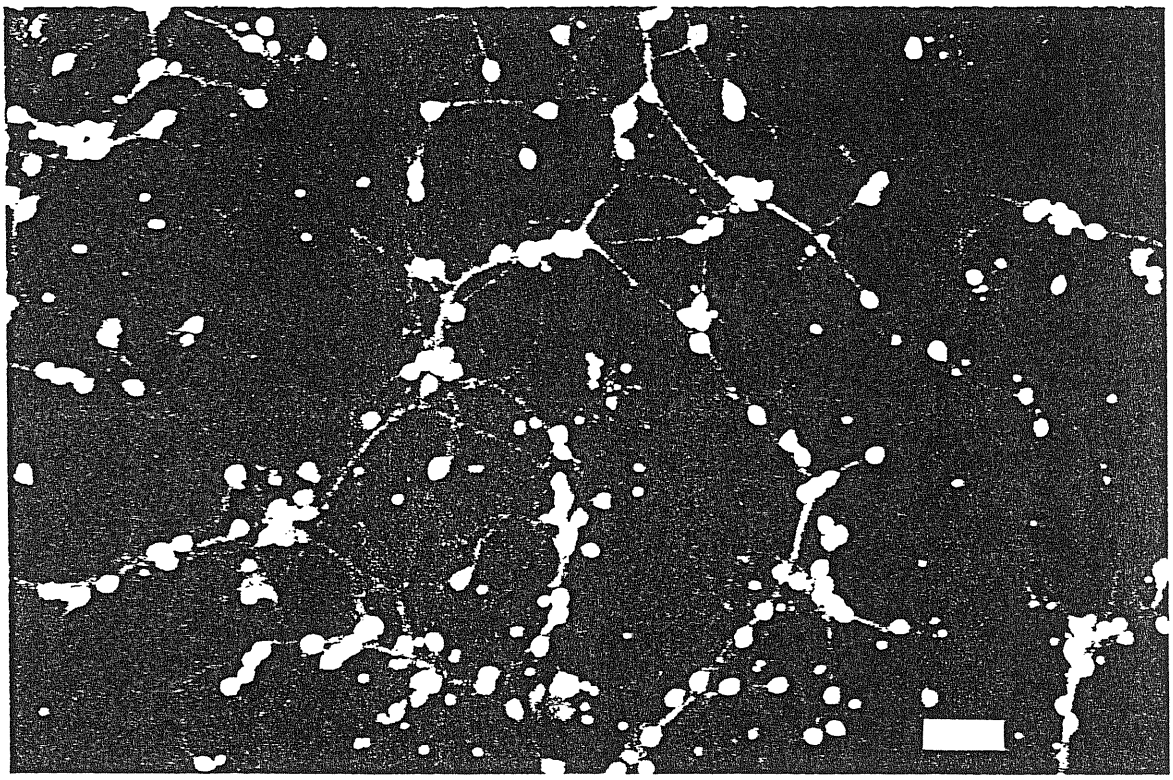

Figure 3.1 Cerebellar granule cells in culture. Primary cultures of cerebellar granule cells (7 DIC) stained with a fluorescein. Notice that neuronal processes at this stage are well developed. Bar = 20 μm.

3.2 Whole-cell and outside-out patch-clamp recordings

The patch-clamp technique was first applied about 20 years ago as a variation of the classical voltage-clamp method (Neher and Sakmann, 1976). It was originally developed to directly measure the current through the single ionic channel. The principle of the method is to electrically isolate a patch of membrane and to record the current flowing through the patch. During recording the potential across the patch is controlled. In brief, this method consists of placing a microelectrode on the membrane to be investigated, with an especially tight contact between the electrode tip and the membrane (the resistance of the contact is of the order of 10^{12} Ω). Therefore using a command circuit to control the membrane potential, the current flowing between the pipette electrode and an external electrode will be the ionic current passing through the ionic channels of the patched membrane. The equivalent electrical circuit of the patch-clamp configuration is shown in Figure 3.2. In order to obtain a good control of the patch potential it is important to make a gigaseal in which the resistance of the seal is much higher than the resistance of membrane patch ($R_s >> R_m$). In this condition it is possible to record the membrane currents produced by opening and closing of single ionic channels. Different manipulations after achieving the tight seal between the pipette and the membrane allow several patch-clamp configurations for specifically required currents recordings, such as the whole-cell current or the single-channel recordings (Figure 3.3; Hamill et al, 1981). Among all the configurations, the *cell-attached* configuration is directly obtained by the formation of the seal between the pipette and the membrane. With this method the cell content is kept intact allowing the study of ionic channels which are sensitive to the metabolic processes of the cell. The other two recording configurations, *inside-out* and *outsie-out*, are obtained by pulling up the

recording pipette before or after disrupting the patched cell membrane. In these two cases, the ionic current recorded is that flowing through this small piece of membrane. These two configurations open the possibility to easily control the "intracellular" or "extracellular" compositions of the patched membrane. The *whole-cell* configuration is achieved by applying a negative pressure or voltage pulses to break the membrane after the cell-attached configuration is formed. Since the direct communication is established between the pipette and the intracellular compartment in the whole cell configuration, the intracellular solution is rapidly dialyzed to the pipette solution, giving a control of the intracellular composition of the patched cell.

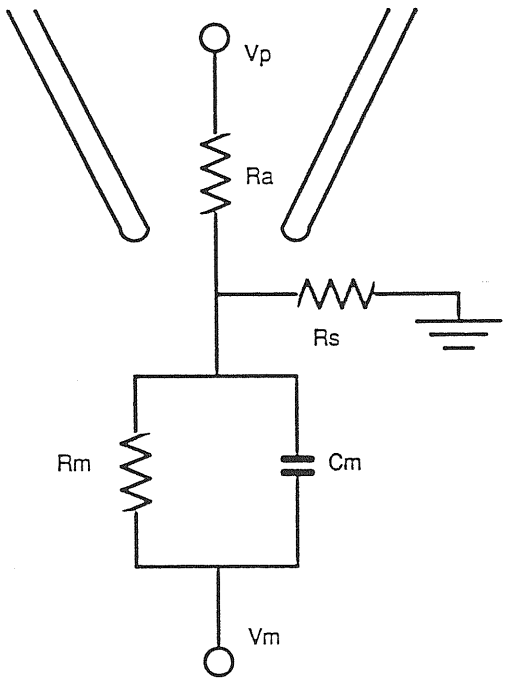

Figure 3.2 Equivalent circuit of the patch-clamp pipette attached to the cell membrane. Measurement of single-channel events can be obtained if the current passing from the pipette interior to the external solution is considerably small in comparison with the current produced by opening of ionic channels in the membrane patch.

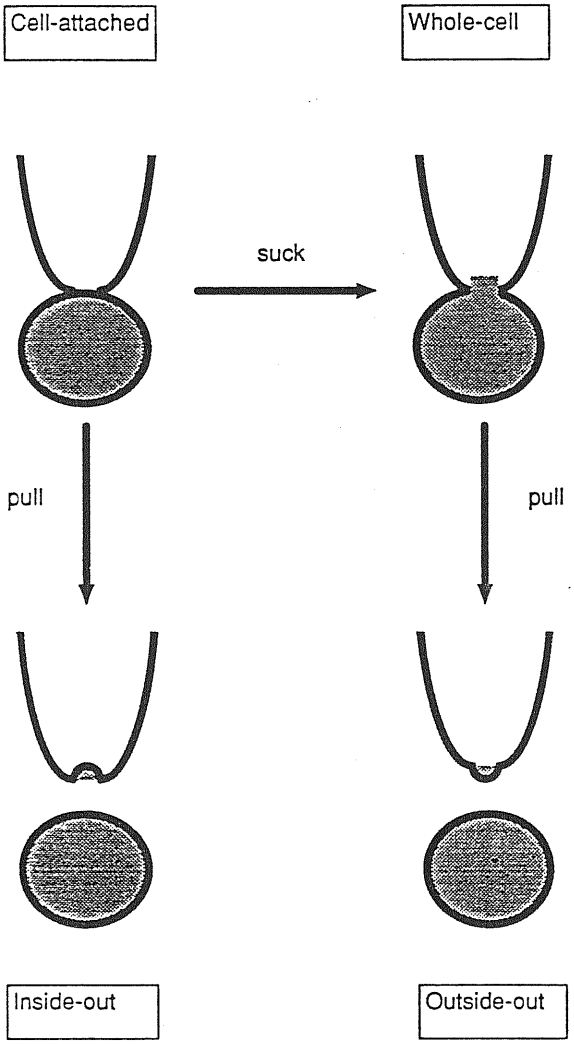

Figure 3.3 Different patch-clamp configurations. (Adapted from Hamill et al 1981).

In the present experiments the recording electrode were made from borosilicate glass capillaries with internal filament (Hilgenberg) pulled with a two stage procedure by a vertical patch-clamp puller (List Medical Electronics). Tips of recording pipettes were fire polished under a microscope. Pipette resistance was in the range of 5-10 MΩ measured in working solutions.

GABA- or glycine-evoked currents were studied using a standard patch clamp amplifier (EPC-7, List Medical Instruments, Darmstadt, Germany). The patch-clamp instruments used in our experiments were organized as in Figure 3.4 (the recording part) and 3.5 (the support part).

The cell dish was mounted on a movable support on a microscope (IM35, Zeiss, FRG) with Nomarski optics. The I-V converter of the EPC-7 was mounted on a three dimensional micro movement manipulator (Micro-Control, France). The final fine movement of recording pipette was controlled by a piezoelectric micromanipulator (Physik Instruments, Germany). The aquisition and electrical stimulation were done using a microcomputer (ATARI 1040ST) after digitization with a 16 bits analogue-digital converter (ITC-16, Instrutech, USA). The operation of converter was controlled by a microcomputer which used a commercial program "Acquire" (Instrutech), written in Modula-2 by H. Affolter from Yale University. The current signal filtered at 10 kHz was directly recorded from one output of EPC-7 on video tape using the combination of Pulse Code Modulator (PCM; Instrutech,USA) and video recorder (VTR). During experiments the current signal was filtered at 2 kHz and simultaneously monitored on an oscilloscope and on the monitor of a microcomputer. Data stored on the tape were filtered at a cut off frequency, as specified later, with a low pass 8-pole Bessel filter (902LPF2, Frequency devices, Haverhill, Massachusetts). Data were digitized and transferred to the microcomputer hard disk at appropriate sampling time. Whole-cell glycine currents were sampled at

100 Hz and filtered at 1 KHz. Spontaneous GABA-mediated synaptic currents were sampled at 1 kHz and filtered at 300 Hz. Single channel currents were sampled at 5 kHz and filtered at 2 kHz.

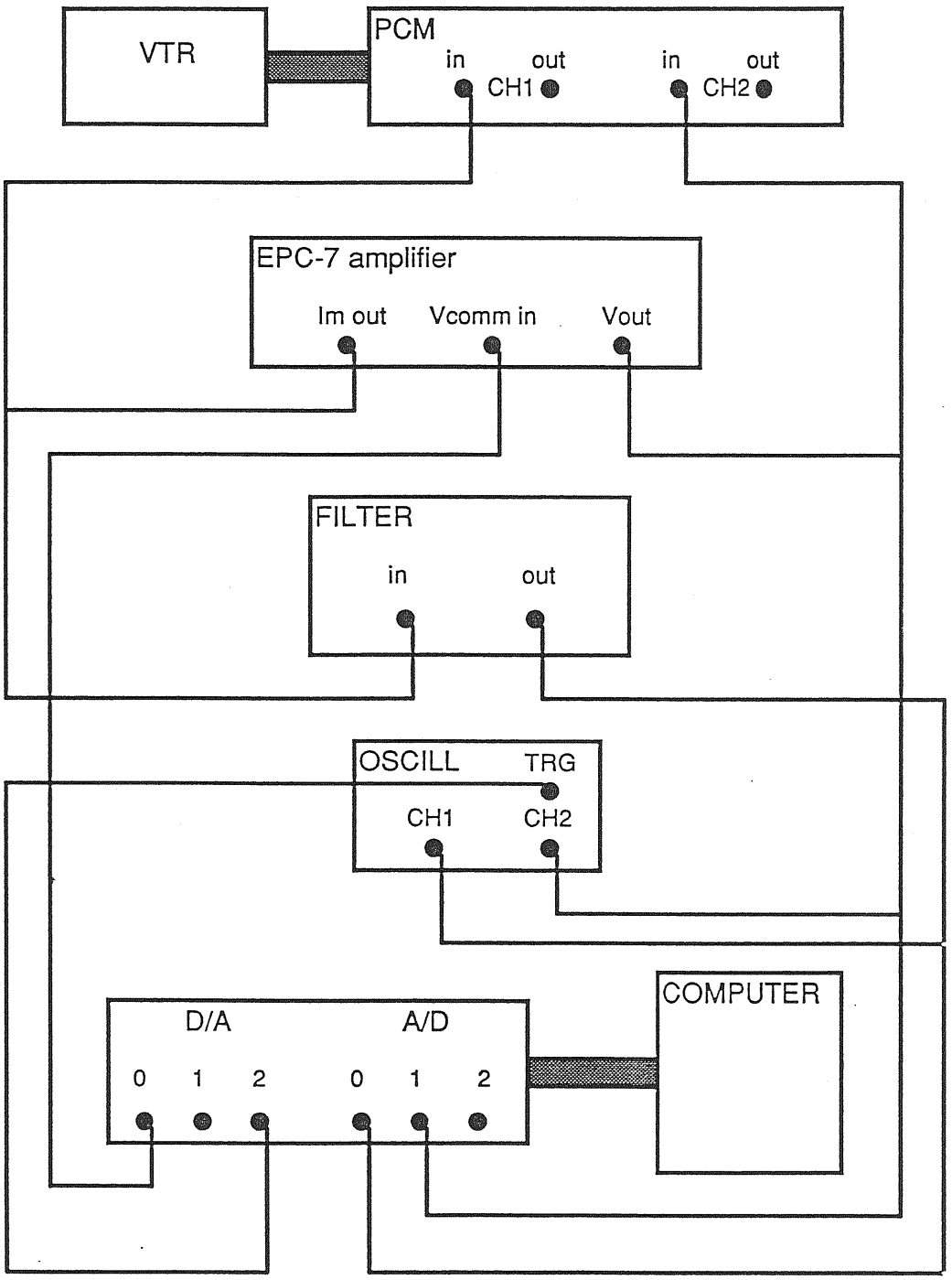

Figure 3.4 Electronic part of the patch-clamp equipment.

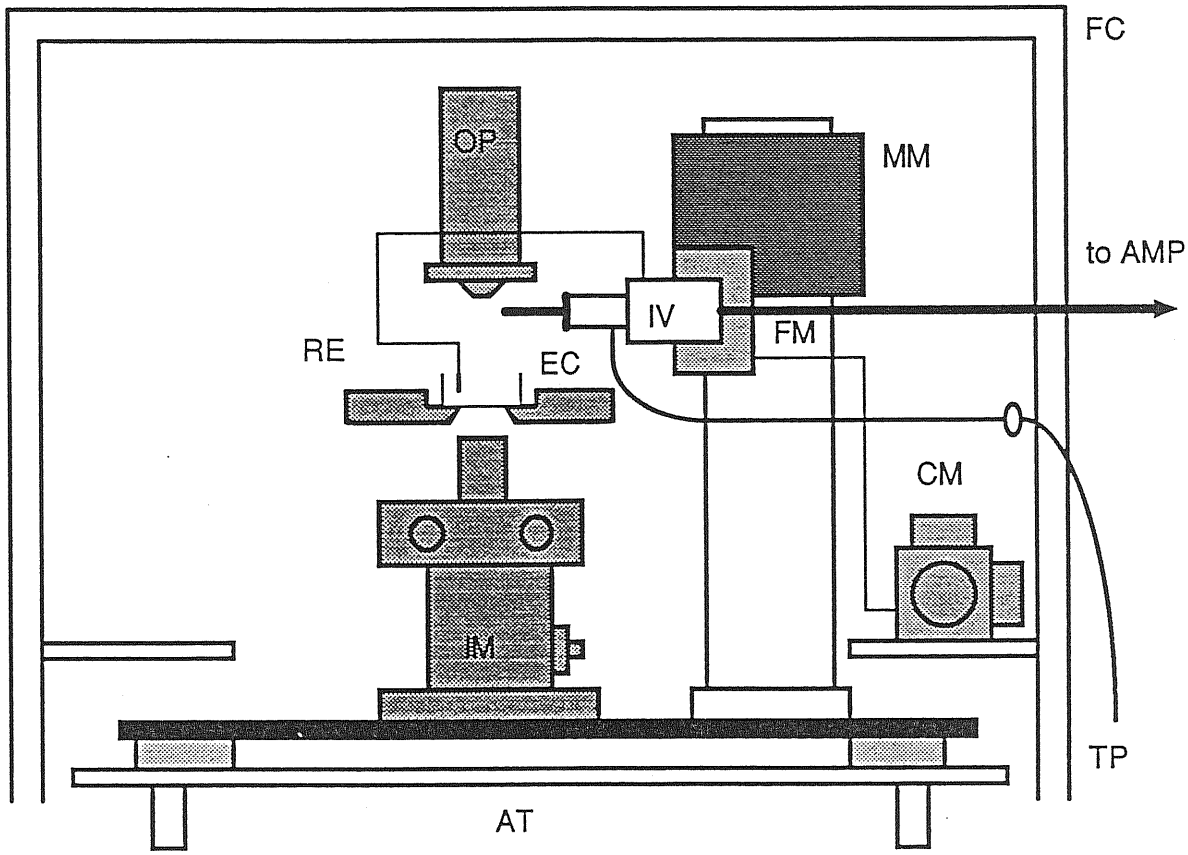

Figure 3.5 Mechanical part of the patch-clamp set up. AMP: Patch-clamp amplifier. AT: antivibratory table. EC: experimental chamber. FC: Faraday cage. FM: fine micromanipulators. IM: inverted micrscope. IV: current to voltage converter. CM: Three dimensional micro movement controller. MM coarse micromanipulators. OP: Microscope optics. RE: Reference electrode. TP: tube for applying pressure.

3.3 Solutions

The solutions used in electrophysiological experiments are shown in Table 1. Pipette and bath solutions were the same for whole-cell and outside-out configurations. The pH of bath and pipette solutions was adjusted to 7.3 with NaOH and CsOH respectively. Some experiments were performed in low extracellular chloride solutions. In these cases, 40 or 90 mM NaCl were substituted with 40 or 90 mM sodium isethionate in order to have a final $[Cl^-]_o$ of 50 or 100 mM, respectively. In these conditions liquid junction potentials resulting from different mobilities of ions at interfaces between solutions having different ionic composition (the electrode and the bathing solution) develop. To avoid this problem in some experiments an agar bridge was used. This consisted of a teflon tube filled with agar. The agar was prepared with the control bath solution in which the concentration of Cl^- ions was close to that of the pipette solution. One end of the agar bridge was immersed in the bath solution and in the other end the ground wire was inserted. In this way the solutions in contact with the silver chloride electrode in the pipette and in the bath (the ground electrode) had the same concentration of Cl^- ions.

High concentration of Cs^+ was present in the pipette solution in order to block most of potassium channels. The presence of Mg^{2+} in the extracellular solution provided a blocker at the negative holding potentials of spontaneous channels which were mainly mediated by glutamate acting on NMDA receptors (Kilic et al, 1991). As mentioned in the introduction glycine receptor subunits contain a consensus sequence for phosphorylation by protein kinase C and A (Ruiz-Gómez et al, 1991 Vaello et al, 1992; 1994; Schönrock and Bormann, 1995) that, as for $GABA_A$-receptors (Stelzer et al, 1988), have a role in the modulation of glycine receptor function. In spinal cord neurons GlyR can be phosphorylated in response to the

presence of either PKC or PKA activators and the stimulation of these transduction pathways leads to a decrease or an enhancement of GlyR functionality respectively (Vaello et al, 1994), while in cultured hippocampal neurons GlyR is positively modulated by PKC (Schönrock and Bormann, 1995). Therefore to prevent eventual run-down of glycine-activated currents due to the loss of cytoplasmic components, ATP and Mg2+ were routinely included in the pipette solution.

Bath	[mM]	Pipette	[mM]
NaCl	140	CsCl	137
KCl	3	$MgCl_2$	4
$CaCl_2$	1.5	EGTA	5
$MgCl_2$	2	$ATP\text{-}Na_2$	2
Hepes-NaOH	10	Hepes-CsOH	10
D-glucose	10		

Table 1. Extracellular (bath) and intracellular (pipette) solutions for whole-cell patch-clamp recordings.

3.4 Drug application

Granule cells were kept at room temperature (22-24°C) and continuously superfused with extracellular (control) solution applied by gravity (at 2 ml min^{-1}) through a barrel. Receptor antagonists or channel blockers such as bicuculline, strychnine or picrotoxin were dissolved in the bathing solution and applied by gravity through a second barrel. The barrels terminated in a small teflon tube (diameter of about 1 mm) located at the periphery of the Petri dish as shown in Figure 3.6. With this application method the equilibrium was reached in one minute. The suction tube

was opposed to the perfusion tube. GABA and glycine were applied by a fast perfusion system, using the Y tube method (Akaike et al, 1991; Figure 3.6). Briefly, the Y tube was made of polyethylene tubing (2 mm o.d.,1.5 mm i.d.) and the outlet tip (0.18 mm o.d., 0.10 mm i.d.) was set at about 200 μm from the patched cell. One end of the tube was placed into a tube containing the test or the control solution; the other end was connected to an electromagnetic valve controlled by an electronic device which allowed the close time setting of the valve. When the valve was opened, the external solution was changed by a negative pressure. When the valve was closed, flow through the Y tube was inverted and the solution was rapidly expelled from the outlet tip for gravity. With this method a complete exchange of the external solution surrounding the neuron was achieved within 100 ms. Drugs used were: glycine, GABA, strychnine, picrotoxin and bicuculline methiodide, all purchased from Sigma.

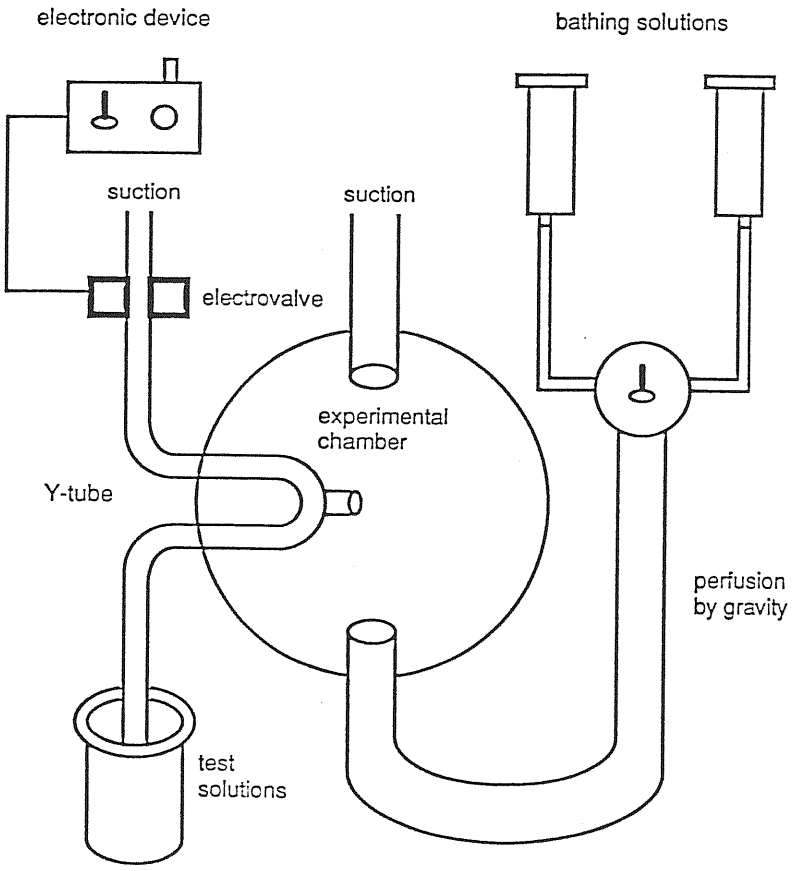

Figure 3.6 Fast perfusion system.

3.5 Data analysis

Whole cell currents were analyzed with the "TAC" program of the Instrutech Corporation (Elmont, N.Y.). Dose-response curves were fitted with the empirical Hill equation:

$$I/I_{max} = 1 / 1 + (K / c)^n \qquad (2\text{-}1)$$

where I is the peak of agonist induced current, I_{max} is the peak of maximal induced current, c is the concentration of the agonist, K is the half-maximum concentration which corresponds to the EC_{50} and n is the Hill coefficient. This and the following fittings were performed in Sigma Plot (Jandel Corporation) which uses a least squares procedure.

A slightly rearranged equation was used to fit dose-response curves for the blockage effect of receptor antagonists or channel blockers in the presence of constant, non saturating concentration of the agonist:

$$I_{ant} / I_0 = 1 / 1 + (K_i / [ant])^{n_i} \qquad (2\text{-}2)$$

where I_{ant} is the peak of agonist induced current in the presence of the antagonist, I_0 is the agonist induced current in the absence of the antagonist, $[ant]$ is the concentration of the antagonist, K_i is the half-maximum blocking concentration of the antagonist which corresponds to the 50% inhibition concentration (IC_{50}) and n_i is the Hill coefficient of antagonist inhibition.

Inactivating currents evoked by neurotransmitters needed time to recover from desensitization before the receptors were able to be activated again. To study the

recovery process a double-pulse protocol was used. In each train of stimuli two identical agonist pulses, separated in time, were applied to the same cell. We estimated the recovery time constant (τ_r) according to the equation:

$$I / I_p = - [exp (-\tau_r / t) + 1] \qquad (2\text{-}3)$$

where I_p is the peak current of the first agonist pulse and I is the peak current of the same pulse applied after the time t from the end of the first.

Single channel currents were analyzed with the TAC program (Instrutech; Sigworth, 1985) which uses 50% threshold criteria in the detection of channel opening and closing. The open and close time histograms were fitted with exponential functions by the method of Sigworth and Sine (1987). The total open time (Np), defined as the product of the number N of channels in a patch and the open probability p for each channel, was calculated as the ratio between the sum of all open times and the total observation time, taking the agonist application as the total observation time. This is true if the openings of separated channels in the patch are indipendent events. Amplitude distribution histograms of single channel openings were fitted, by eye, with the sum of Gaussian functions using the same program.

Current-voltage relationship for whole-cell or single channel currents was described by a first grade equation as follows:

$$I = m V + q \qquad (2\text{-}4)$$

where I is the peak current for whole cell recordings or the mean value of the Gaussian used to fit single channel amplitude histograms at different membrane

voltages *V*. The value *m* is the slope and *q* is the intercept on y axis of the straight line. The reversal potential value was obtained from the operation:

$$E_r = -q / m \qquad (2\text{-}5)$$

For single channel experiments the slope conductance coincided with *m*.

Open and close time histograms were fitted with the sum of two exponential curves using the least squares method.

Student's paired and unpaired *t*-tests were used for comparison of paired and unpaired data respectively. Results are usually expressed as mean $\pm$ S.E.M.

Chapter 4

Results

4.1 Glycine evoked whole-cell currents

In this paragraph the electrophysiological and pharmacological properties of currents evoked by glycine in primary cultures of cerebellar granule cells have been studied.

4.1.1 Dose-response

Fast application of glycine to cerebellar granule cells between two and fourteen days in culture (DIC), at a holding potential of -60 mV elicited inward currents in 50 % of the neurons. Although there was a considerable variability in the amplitude of the responses from cell to cell even within the same culture plate, in the same cell the amplitude of the responses was concentration dependent. The minimum effective dose for glycine was 30 μM. Figure 4.1A shows whole cell currents elicited by increasing concentrations of glycine (from 30 to 300 μM). Glycine-induced currents increased steeply as the agonist concentration increased. The mean peak current amplitude elicited by glycine (300 μM), at a holding potential of -60 mV, was 124.9 ± 17.49 pA (n=71). A nearly maximal response was obtained with 1 mM of glycine. Decline of the responses during continuous agonist application was observed only at glycine concentration higher then 30 μM. The affinity and stoichiometry of glycine binding to its receptors can be studied using electrophysiological means by measuring the peak amplitudes of glycine-activated whole-cell currents as a function of glycine concentration. The relationship between the peak current amplitude recorded at -60 mV and agonist concentration is

represented in Figure 4.1B. All responses were normalized to the peak current induced by 1 mM of glycine and plotted against the logarithm of glycine concentration. Data points were fitted with the empirical Hill equation (2-1). The K, corresponding to the concentration of glycine producing half maximum response was 72.8 ± 2.5 μM. The Hill coefficient was 1.6 ± 0.1 suggesting that more than one molecule of glycine is required for opening the channel.

In our experimental conditions, with 2 mM ATP in the recording pipette, we failed to observe any run down of glycine evoked currents. This is shown in Figure 4.2 where glycine (300 μM) was repetitively applied every 3 minutes for 15 minutes.

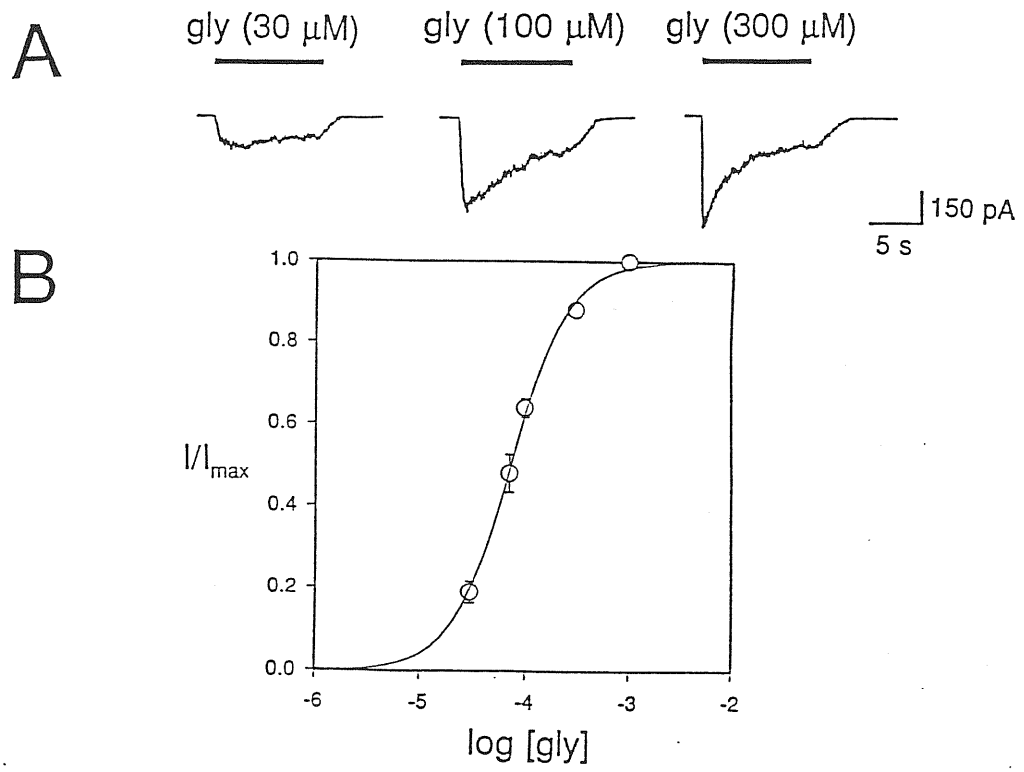

Figure 4.1 Concentration-response relationship of glycine-evoked currents. A. Whole cell currents evoked by application of increasing concentrations of glycine (closed bars) at a holding potential of -60 mV. Desensitization of glycine responses occurred with concentration of the agonist higher than 30 μM. B. Plot of the peak amplitude of glycine currents normalized to those evoked at 10^{-3} M glycine versus agonist concentrations. Each point represents the mean of 29 observations. Bars are the SEM. The continuous line is the best fit to the empirical Hill equation.

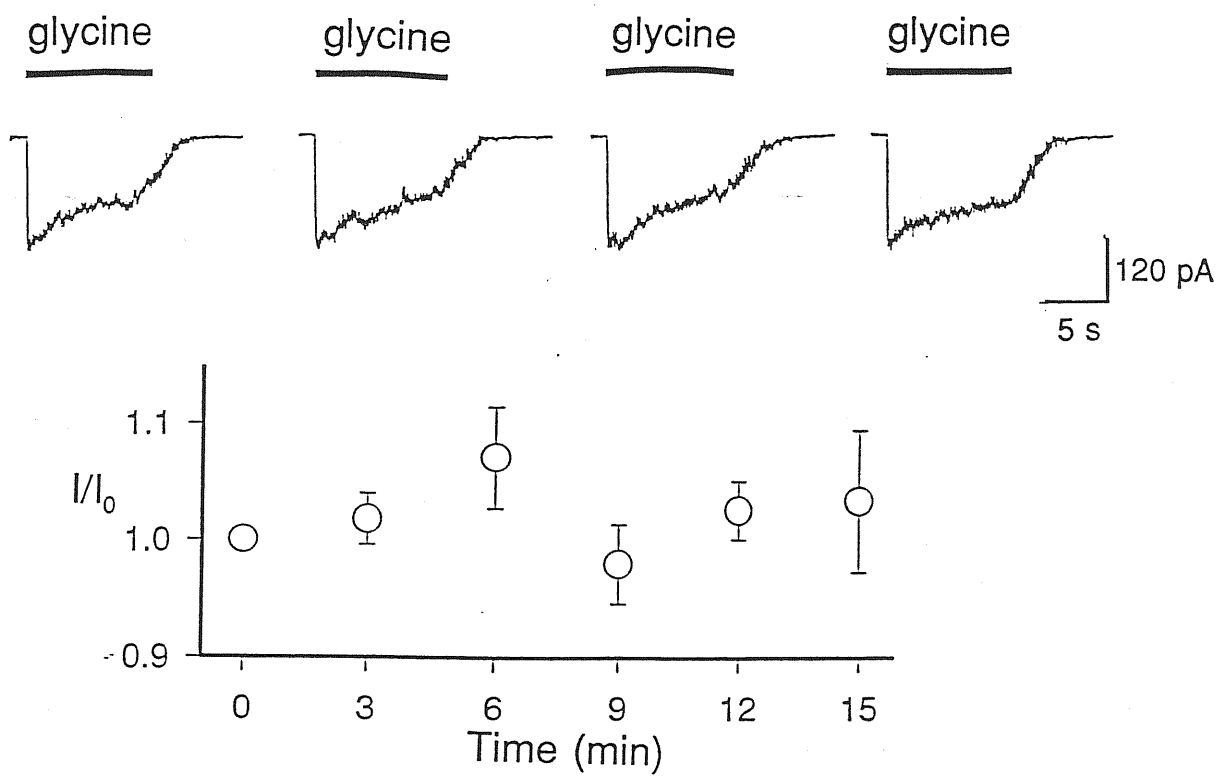

Figure 4.2 Stability of glycine evoked currents. Currents were evoked at 3 minutes intervals and their peak amplitude, expressed as a percentage of the current evoked by the first application of glycine, were plotted versus the time. Each point represent the mean value of 4-8 observations. Bars are the SEM.

4.1.2 Current-voltage relationship

Figure 4.3A shows a family of currents evoked by glycine (300 μM), in nearly symmetrical Cl^- solutions ($[Cl]_o$ 150 mM) at a holding potential of -20, 0 and 20 mV. These currents were inward at negative potentials, their amplitude decreased with membrane depolarization and became outward at potentials more positive than 4.9 ± 0.9 mV (n=14) a value close to the predicted Cl^- equilibrium potential (-0.86 mM), calculated from Nernst equation in our recording conditions. The relationship between amplitude of the current and membrane potential (Figure 4.3B, diamonds) was linear in the potential range between -40 to 40 mV. As shown in the same Figure, in six cells decreasing $[Cl]_o$ from 150 (diamonds) to 100 (circles) and 50 (triangles) mM (isethionate substitution) caused the reversal potential for

glycine (E_{gly}) to shift to more positive voltages (10.4 ± 0.8 mV and 27.1 ± 0.5 mV, respectively). These values were very close to those predicted by the Nernst equation. A three fold change in $[Cl^-]_o$ yielded a change in E_{gly} of 22 mV (Figure 4.3C), indicating that glycine conductance is highly permeable to chloride ions.

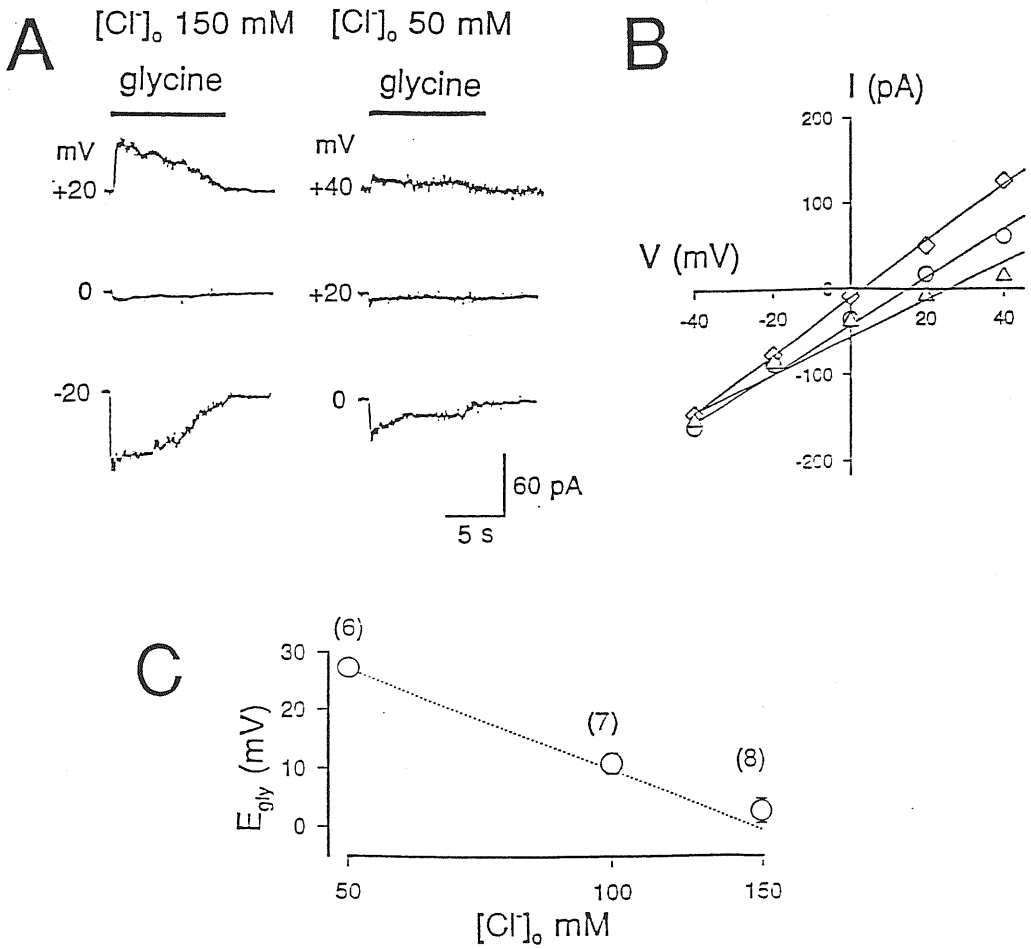

Figure 4.3 Current/voltage relationship of glycine-evoked currents. A. Whole cell currents evoked by glycine (300 µM, closed bars) at various holding potentials, in the presence of 150 mM (left) or 50 mM (right) of $[Cl^-]_o$ (isethionate substitution). B. Peak amplitude of glycine activated currents evoked in 150 (diamond), 100 (circles) or 50 (triangles) mM of $[Cl^-]_o$ (shown in A) are plotted as a function of the holding potential. The I/V relationship was linear in the potential range from -40 to 40 mV. C. Relationship between the reversal potentials of glycine-induced currents (E_{gly}) and $[Cl^-]_o$. Each point represents the mean and SEM obtained in six cells. The dotted line correspond to the values of the reversal potential for chloride ions calculated from the Nernst equation in different $[Cl^-]_o$.

4.1.3 Desensitization

As already mentioned, decline of the response during continuous glycine application was concentration dependent. In fact with a low concentration of glycine (30 μM) the current decline was not detectable, whereas with high dose of glycine (300 μM) the decline progressed rapidly (Figure 4.1A). In Figure 4.4A the ratio between I_{peak} / $I_{steady\text{-}state}$ of whole cell glycine currents elicited at a holding potential of -60 mV, versus different agonist concentrations is plotted. As shown in the Figure, the peak to plateau ratio shifted from 1.1 ± 0.05 to 2.1 ± 0.13 when glycine concentration was enhanced from 3 X 10^{-5} to 1X10^{-3} M, respectively (n=18). The ratio between I_{peak} / $I_{steady\text{-}state}$ was voltage independent in the potential range from -60 mV to 60 mV (Figure 4.4B). For glycine (300 μM) the ratio was 2.1 ± 0.3 at -40 mV and 2.2 ± 0.2 at 40 mV (n=10). The values of the decay time constant (τ_d) of glycine-evoked currents (300 μM) were similar at different holding potentials. At -40 mV and 40 mV τ_d values were 3 ± 0.6 and 3.2 ± 1.7 s, respectively (n=5).

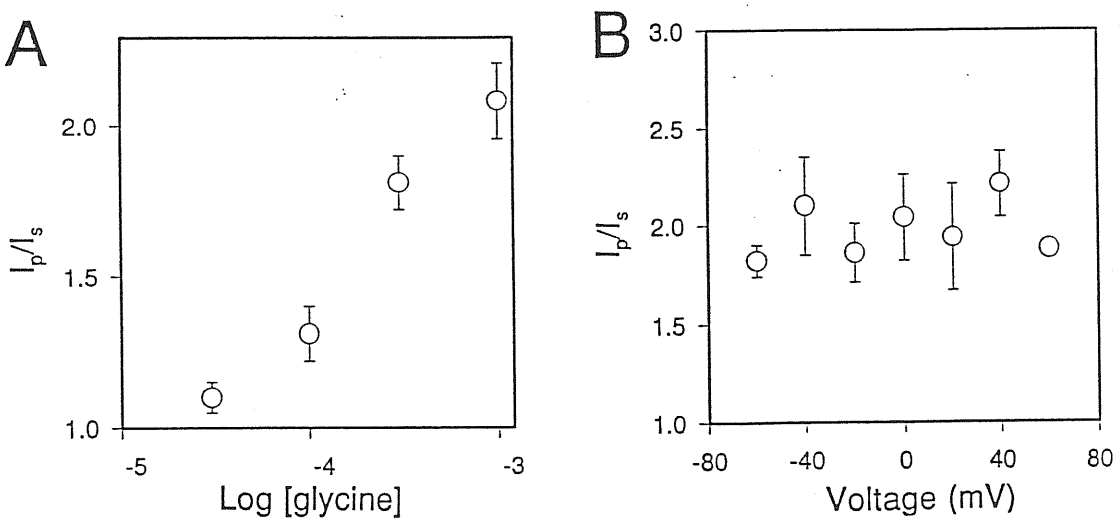

Figure 4.4 Desensitization of glycine-induced currents is concentration dependent and voltage independent. A. Plot of the peak (I_p) to plateau (I_s) ratio of whole cell currents evoked by different glycine concentrations. Each point represents the mean of 18 observations. B. Plot of the peak to plateau ratio of currents evoked by glycine (300 μM) versus different holding potentials. Each point represents the mean of 10 observations. In A and B, bars are the SEM.

4.1.4 Recovery from desensitization

To further characterize glycine-evoked responses, the recovery from desensitization was studied by applying pairs of glycine pulses (300 μM) separated by different time intervals. At a holding potential of -60 mV the recovery from desensitization was relatively fast being completed in 30 sec (Figure 4.5). In Figure 4.5B, the peak amplitude of the response to the 2nd application of agonist normalized to that of the 1st application is plotted versus the time interval between the end of the first and the onset of the second response. Data points were fitted with a single exponential function (2-3) obtaining a time constant of 5.05 ± 0.21 s (n=10).

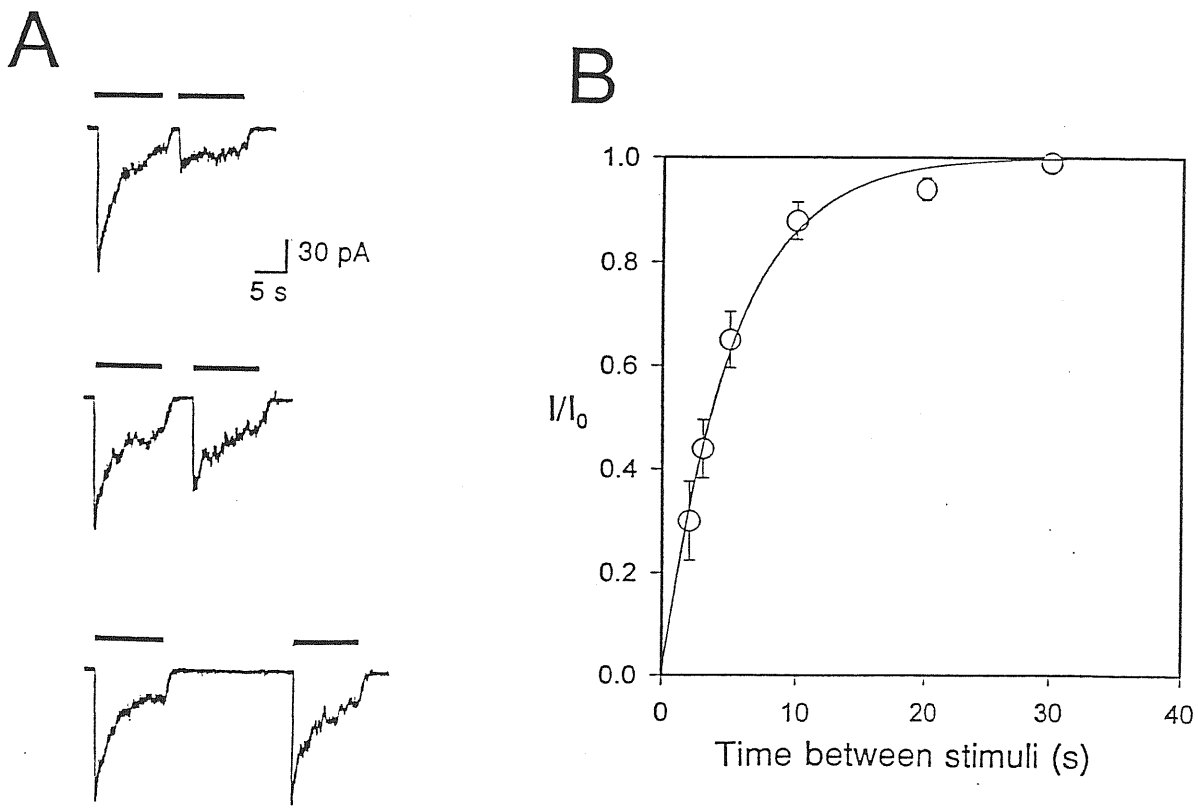

Figure 4.5 Recovery from desensitization of glycine-evoked whole cell currents. A. Pairs of glycine pulses (300 μM, closed bars) separated in time by 2 (upper), 5 (middle) or 20 (lower trace) s. B. Recovery from desensitization, expressed as the ratio I/I_0 versus interstimuli intervals. I_0 represents the peak amplitude of the conditioning glycine response and I the peak amplitude of the test response. The best fitting of the data was obtained with a single exponential having a time constant of 5.1 ± 0.2 s. Each point represents the mean of 10 observations. Bars are the SEM.

4.1.5 Antagonists

The convulsant alkaloid strychnine is considered a selective antagonist of glycine receptors (Curtis et al, 1968). This substance reversibly blocked the response to glycine in a concentration-dependent manner by binding on a site of the N-terminal extracellular region that may also be involved in forming part of the glycine binding site (Pfeiffer et al, 1982; Graham et al, 1983; Grenningloh et al, 1987; Ruiz-Gómez et al, 1990; Vandenberg et al, 1992). An almost complete block was achieved by strychnine at 1μM. In Figure 4.6A whole cell currents evoked by application of 200 μM glycine in the absence or presence of two different concentrations of strychnine. Whole cell currents evoked by this non saturating concentration of glycine (200 μM) in the presence of increasing concentrations of strychnine and normalized to the control response were plotted versus the logarithm of different strychnine concentrations (Figure 4.6C). Data points were fitted with the empirical Hill equation (2-2). The half inhibition dose of strychnine (IC_{50}) was 57.9 ± 3.9 nM (n=7). A parallel shift to the right of the dose-response curve for glycine was obtained in the presence of strychnine (100, 300 nM) suggesting, as expected, a competitive action of this antagonist (not shown).

The response to glycine was also antagonized by picrotoxin, a chloride channel blocker, in a dose-dependent manner (Figure 4.6B and D). Picrotoxin however was at least three orders of magnitude less potent then strychnine. The IC_{50} value for picrotoxin was 172.1 ± 0.21 μM (n=5).

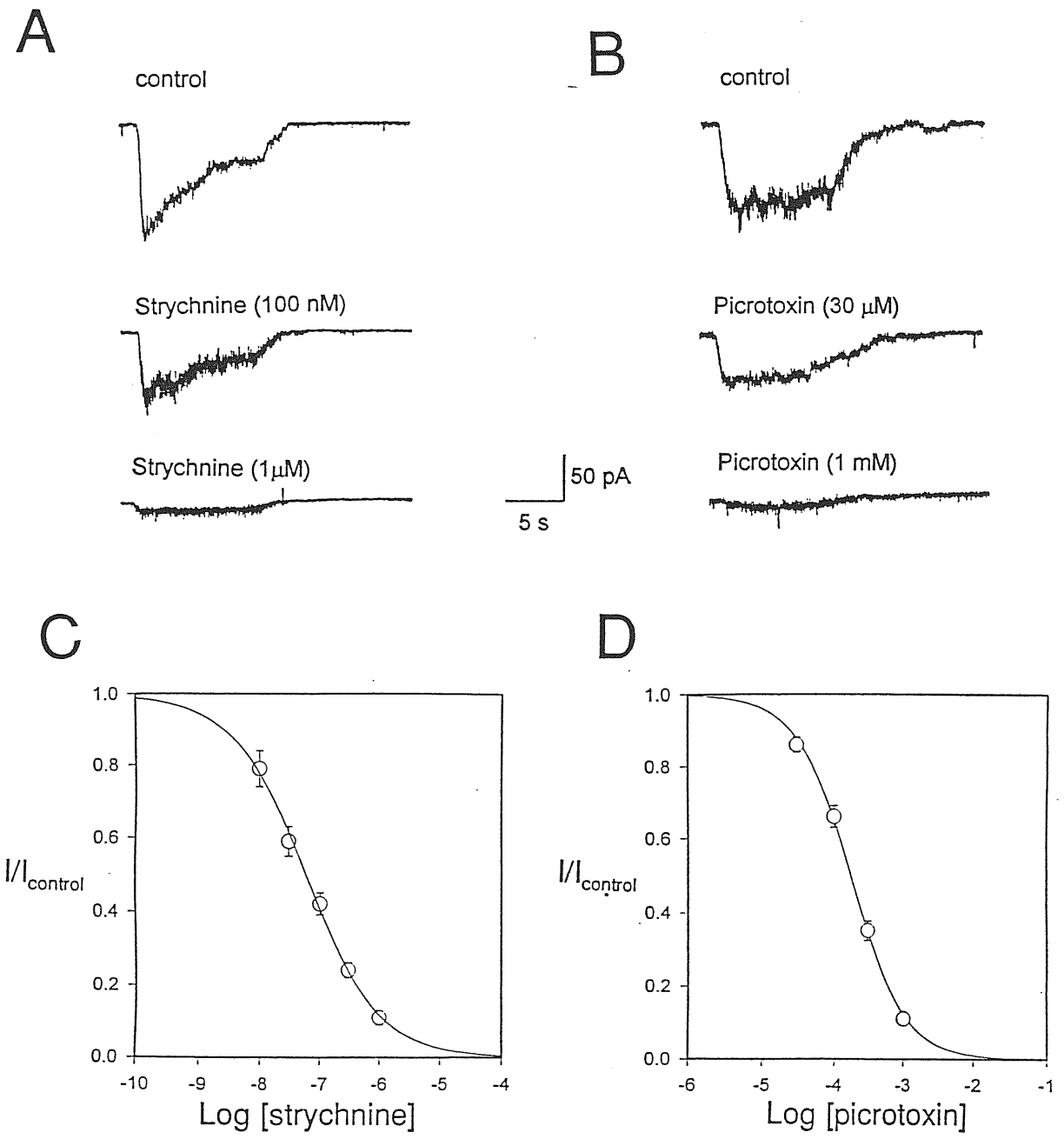

Figure 4.6 Glycine currents are antagonized by strychnine or picrotoxin. Whole-cell currents evoked by application of 200 μM glycine in the absence or presence of two different concentrations of strychnine (A) or picrotoxin (B). C. Dose/response curve for the inhibitory action of strychnine on the peak current amplitude induced by glycine (200 μM). Holding potential was -60 mV. Currents evoked in the presence of strychnine were normalized to those obtained in the absence of the alkaloid. Data points were fitted with the empirical Hill equation. Half maximal block was achieved with a concentration of strychnine of 58 nM. Each point represents the mean of 7 observations. Bars are the SEM. D. Dose response curve for the inhibitory action of picrotoxin on the peak amplitude of glycine evoked currents (200 μM). Glycine currents evoked in the presence of increasing concentrations of picrotoxin were normalized as in C. Data points (from 5 observations) were fitted as in C. Half maximal block was achieved with a concentration of picrotoxin of 172 μM.

4.1.6 Modulation by extracellular zinc

Glycine currents were further characterized by their ability to be modulated by zinc. In fact this divalent cation is present in the brain, stored in synaptic vesicles from which it can be released upon nerve stimulation (Smart et al, 1994). The clearest and most quoted example of a zinc-containing nerve fibre pathway is the mossy fibre projection running from the granule cell layer in the hippocampus to the pyramidal neurons of the region CA3 (Slomianka, 1992). There are many other nerve fibres that contain zinc: some of them are local fibres and others project between identifiable CNS structures. Histological staining for zinc containing fibres has been detected in the hypothalamus, brain stem and cerebellum (Faber et al, 1989; Perez-Clausell et al, 1989; Frederickson, 1989). Moreover in zinc-deficient rats the cerebellum as well as the whole brain is reduced in size. In particular the cerebellar cortex appears underdeveloped and shows a persistence of the external granule cell layer, a reduction in the thickness of molecular layer and a decrease in the area of the internal granule cell layer (Dvergsten et al, 1983).Furthermore extracellular zinc modulates glycine-induced whole-cell currents of cultured spinal neurones, of *Xenopus* oocytes expressing α1, α2 or α1/β glycine receptor subunits (Laube et al, 1995) and of chick ciliary ganglion neurons (Zhang and Berg, 1995). Co-application of zinc (in the range of 0.1-100 μM) and glycine (200 μM) to granule cells in culture induced a potentiation of glycine-evoked currents. This effect was concentration dependent and was reversible upon 5 minutes of wash out (Figure 4.7). Zinc (100 μM) potentiated the peak of glycine currents by 24.1 ± 7.4 % (n=6) in a reversible way. The concentrations of zinc used here are comparable with those employed by Laube et al (1995) and Zhang and Berg (1995).

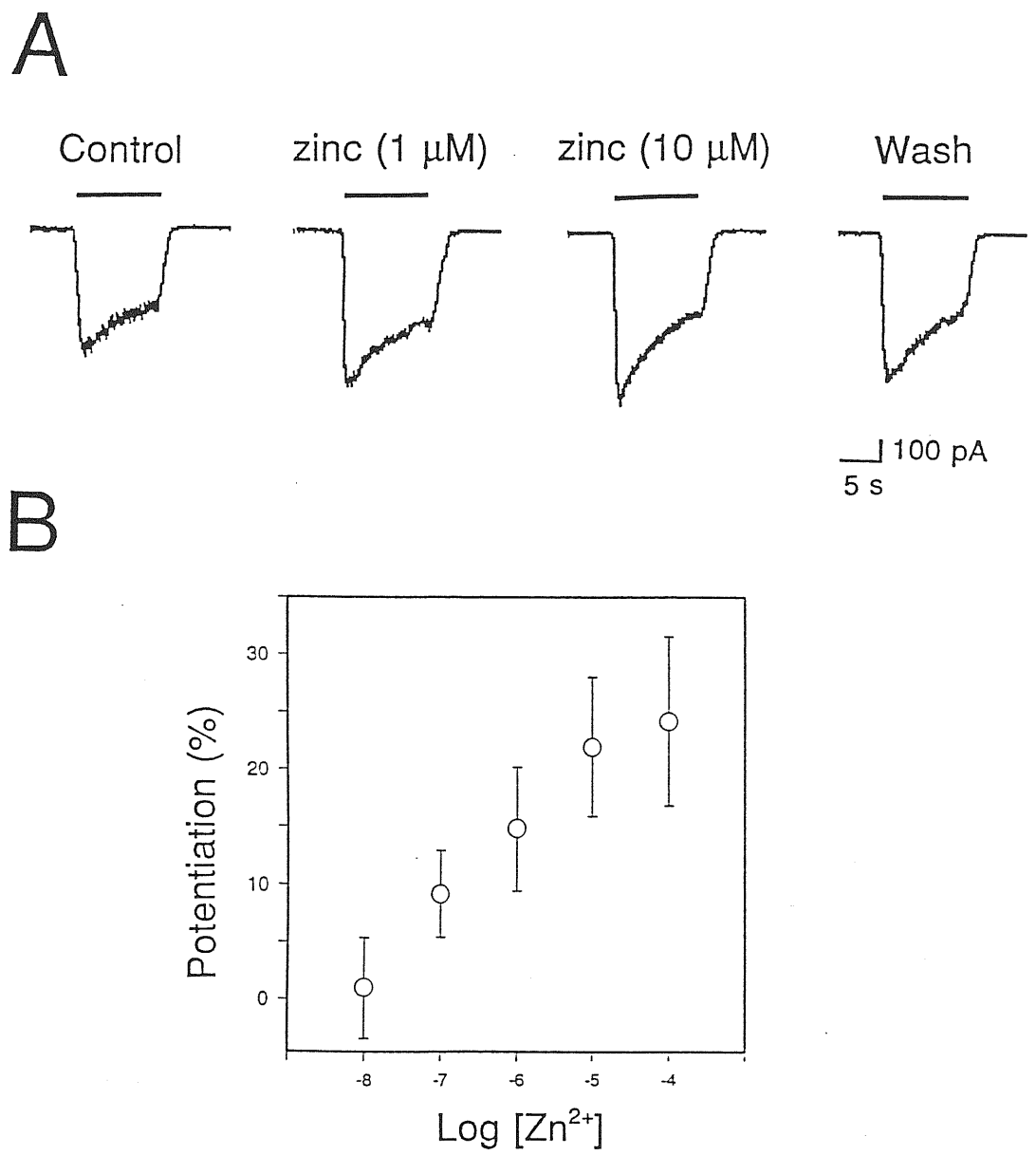

Figure 4.7 Potentiating effect of zinc on glycine currents. A. Currents evoked by glycine (200 μM, bars) at a holding potential of -60 mV in the absence or in the presence of 1 and 10 μM zinc. B. Plot of the percentage of potentiation of the peak amplitude glycine currents versus zinc concentration. Each point represents the mean of six responses. Bars are the SEM.

4.1.7 Glycine and GABA act on distinct receptor channels: antagonist specificity

To see whether the depressant effect of strychnine was selective for glycine, both strychnine and bicuculline were tested on the responses induced on the same neuron by fast application of glycine or GABA. Strychnine (1 μM) antagonized the response to glycine but had no effects on GABA-evoked current (300 μM, n=2). In contrast, bicuculline (100 μM) strongly depressed GABA responses without affecting glycine-induced currents (300 μM, n=7, Figure 4.8). The selective block of glycine or GABA currents by strychnine or bicuculline respectively suggests the involvement of two different receptors. It was therefore interesting to further examine whether these amino acids in turn activated separate channels with different properties. If we asssume that GABA or glycine activate different conductances, a saturating concentration of glycine should give a response not occluded by co-application of GABA and viceversa. A typical experiment is represented in Figure 4.9. When GABA (3 μM) was applied together with a saturating concentration of glycine (1 mM), the conductance increase produced by the two agonists was additive. Moreover, no cross desensitization was observed when GABA was applied during glycine desensitization. Similar results were obtained in eight additional experiments. These data clearly indicate that GABA and glycine activate two different populations of ion channels.

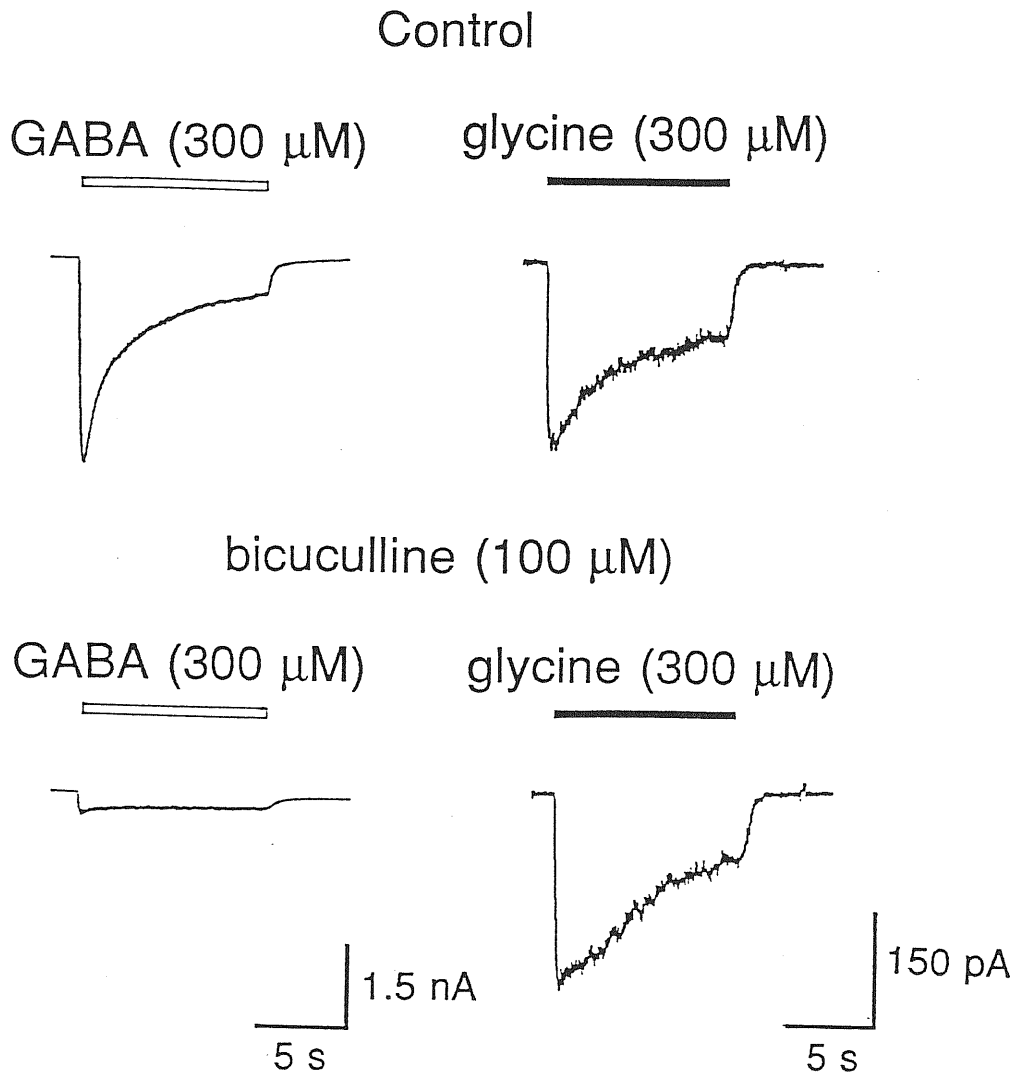

Figure 4.8 Glycine evoked current is not blocked by the specific GABA antagonist bicuculine. Bicuculline (100 μM) strongly depressed GABA currents activated by 300 μM GABA, whitout affecting glycine induced currents (300μM).

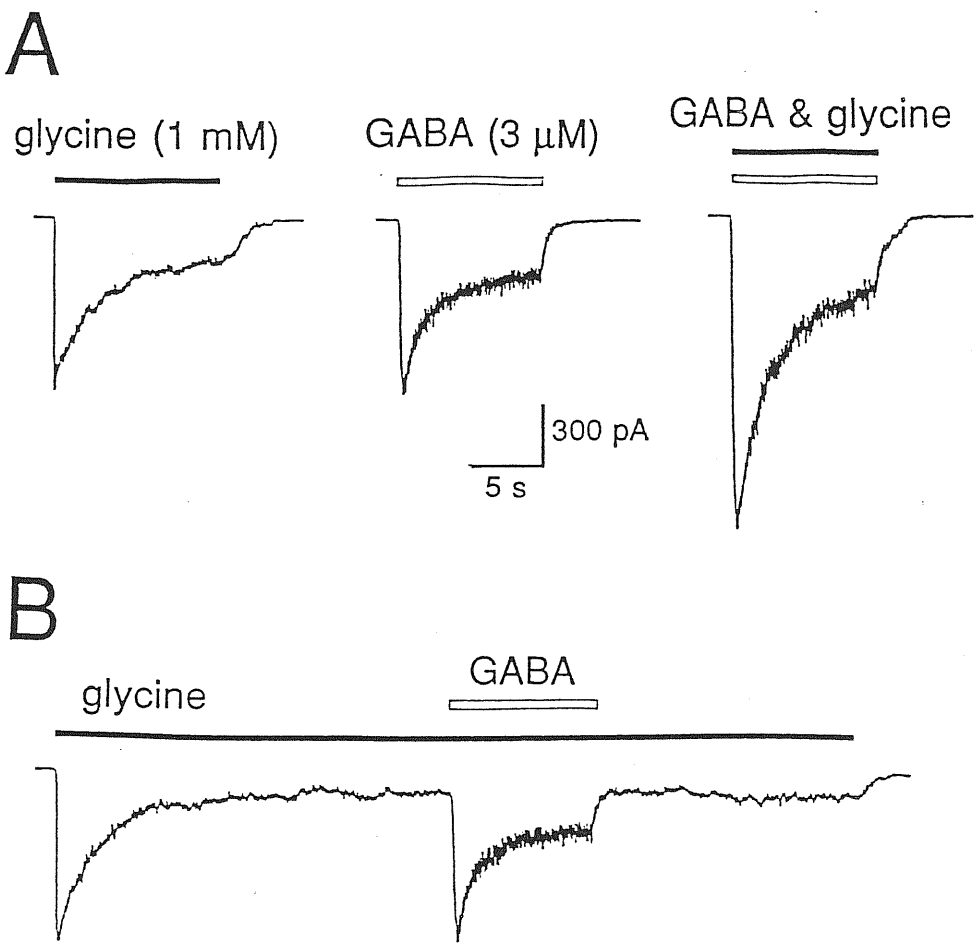

Figure 4.9 GABA and glycine activate different populations of receptor channels. A. The cell was held at -60 mV. GABA (open bar) and glycine (closed bar) were applied either separately or in combination. When applied together, the current induced by glycine summed to that produced by GABA. B. Application of glycine for about 1 min, induced an inward current that after an initial peak desensitized to a plateau level. Superfusion of GABA during the plateau phase produced a response similar to that induced by GABA in the absence of glycine, suggesting that no cross desensitization between the two agonists was present.

4.2 Glycine-activated single channel currents

Glycine-activated single channel currents were studied in excised patches. Single channel events were recorded in outside-out patches which contained less than three channels.

4.2.1 Conductance levels

In preliminary experiments from six excised, outside-out patches the responses to glycine were studied at the single channel level. No openings were observed in the presence of the control solution. At a holding potential of -40 mV, bath application of glycine (in the range of 30-300 μM) activated single channel currents of different amplitudes. The single channel events were reversibly blocked by strychnine (1 μM), suggesting that they were mediated by activation of glycine receptors (data not shown). In 2 cases the amplitude distribution of glycine gated channels were fitted with the sum of three Gaussian curves. Chord conductance values, estimated from the driving potential (-40 mV), were 28.5 ± 2.3 pS (n = 3), 52.5 ± 1.8 pS (n = 5) and 85.5 ± 5.25 pS (n = 2, Figure 4.10A). Figure 4.10B shows a typical amplitude distribution histogram of glycine (100 μM, for 100 s) evoked single channel events at -40 mV. When the three conductance channels were present on the same cell, the most frequently occurring one was the 52.5 pS (relative frequency 21 and 57%). The amplitude of single channel currents measured at different holding potentials was plotted versus different voltages. As for whole cell currents, single channel I/V relationship was linear in the potential range -60, 60 mV suggesting that the pore of glycine-receptor channel does not change the permeability for Cl^- at the voltages examined. Conductances, estimated from the slope of the I/V curves were 31, 53 and 84 pS (Figure 4.10C).

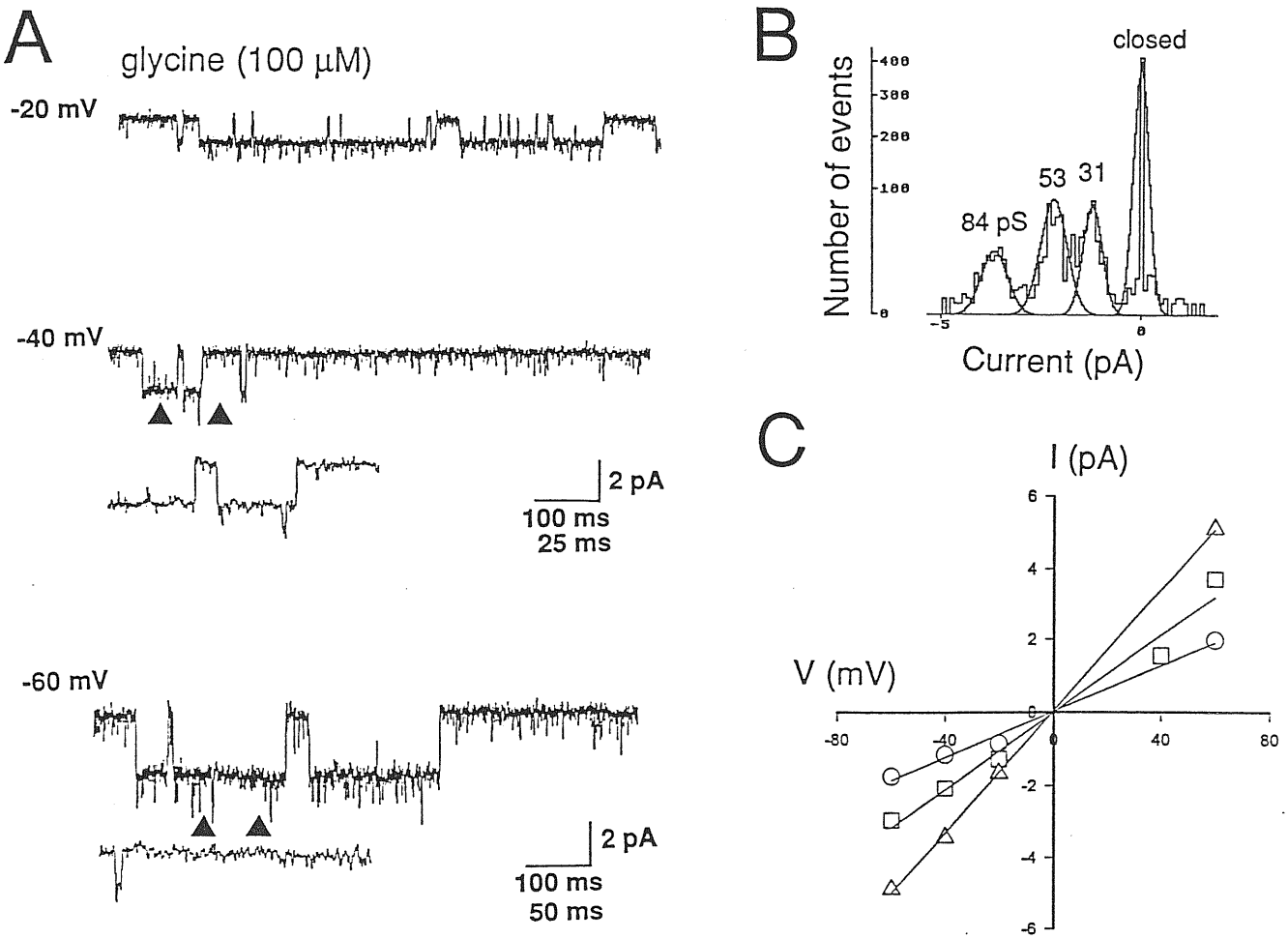

Figure 4.10 Single channel currents activated by glycine. A. Representative traces of single channel currents activated by glycine in an outside-out membrane patch at different holding potentials. Traces were digitized at 5 kHz, after low-pass filtering at 1 kHz. Expanded portions of one traces (between arrows) is shown. B. Amplitude distribution histogram of single channel currents recorded at -40 mV (see A). C. Single-channel current-voltage relationship for the same cell. Experimental data were fitted by least-squares linear regressions, yelding slope conductances of 31 pS (circles), 53 pS (squares) and 84 pS (triangles).

The different channels exhibited different kinetic properties. The 53 and 84pS channels showed prolonged openings while the 31 pS showed brief and more frequent openings (see Figure 4.11A). In two cells only the 31 and 84 pS conductance states were observed (Figure 4.11A), suggesting a different stoichiometry of the subunits in the receptor channel and/or different subunit composition. Because the most frequent single channel event was the 53 pS one, the kinetic properties of this channel have been studied in more detail. The opening frequency of this channel was concentration dependent. Outside-out patches were exposed to 30, 100 and 300 μM glycine at a holding potential of -40 mV and channel activity was quantified by measuring Np, as already described in chapter 3. As shown in Figure 4.12, raising glycine concentraton from 30 to 300 μM, induced a 2.2-fold increase in Np.

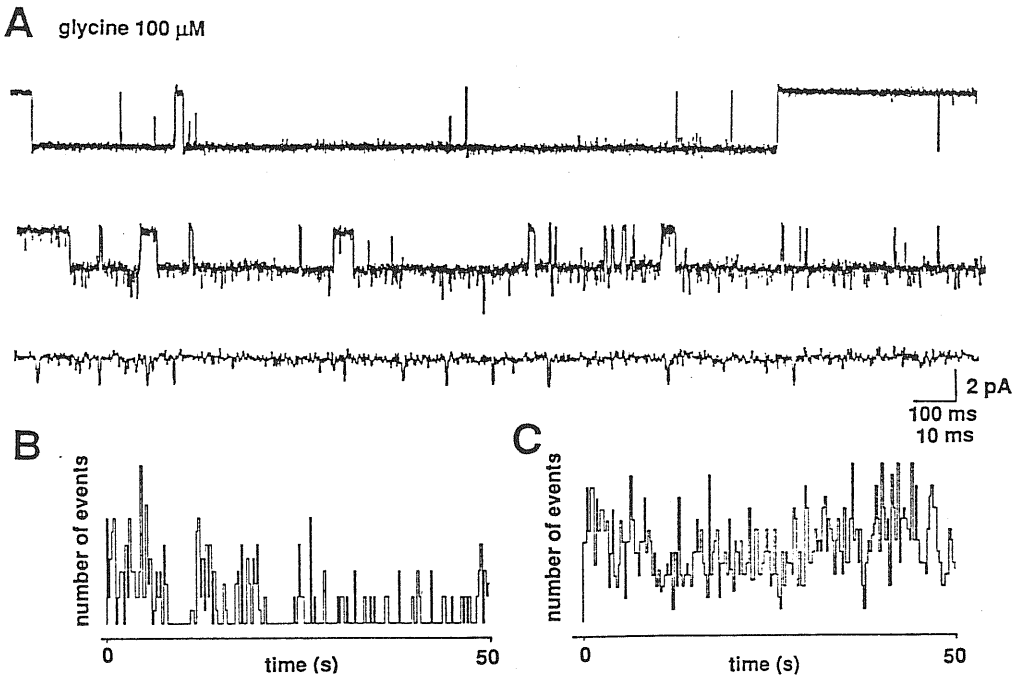

Figure 4.11 Glycine gated single-channel currents. A. Examples of the 84 pS (upper trace), 53 pS (middle trace) and 31 pS (lower trace) conductances. The single channel currents were evoked by 100 μM glycine at a holding potential of -40 mV. Trace are from three different neurons. B and C. Time course of single channel openings for the 53 pS (B) and 31 pS (C). Note the desensitization of the 53 pS channel. Each bin = 250 ms.

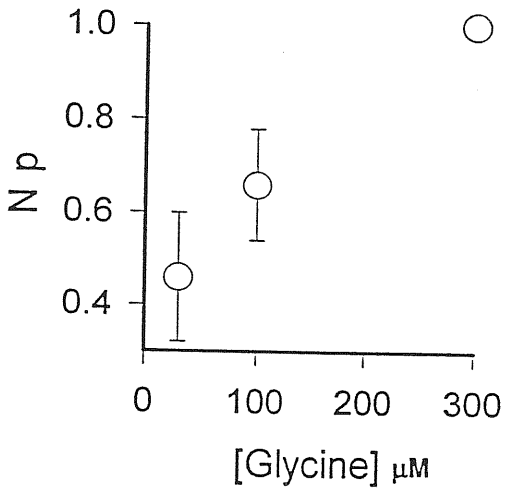

Figure 4.12 Probability of single channel opening increase with glycine concentration. The open channel probability, Np, was plotted as a function of glycine concentration. Np measured in the presence of 30 and 100 μM glycine was normalized with respect to the value obtained with 300 μM. Data points represent the average of 3 patches. Bars are SEM.

4.2.2 Kinetic analysis

In Table 2 are summarized the open, closed and burst time constants of single channel events activated at -40 mV by two concentrations of glycine (30 and 300 μM). In the presence of 30 μM glycine, open time histograms could be fitted with the sum of two exponential curves having time constants (τ) of 0.9 and 140 ms (n = 4). Similarly, in the presence of 300 μM glycine, open time histograms could be fitted with the sum of two exponential curves having τ of 1.6 and 160 ms (n = 6; Figure 4.13A. These values were not significantly ($p > 0.1$) different from those obtained in the presence of 30 μM glycine. As the open time values also the relative weights, or exponential areas, were similar in both experimental conditions.

The closed time histograms obtained with glycine 30 μM could be fitted with the sum of two exponentials having time constants of 12 and 2700 ms (n = 4). In the presence of 300 μM glycine closed time histograms could also be fitted with the sum of two exponential curves having τ of 4.7 and 1790 ms (n = 7; Figure 4.13B). The fast closed time constants of single channel events obtained in 30 and 300 μM glycine were significantly ($p < 0.01$) different. Furthermore the relative contribution of the fast and slow closed time constants was different in the two experimental conditions: the relative contribution of the fast component decreased, while that of the slow component increased at higher glycine concentration. It is possible that we overestimated the value of τc_2 because of the partial desensitization of agonist induced response as shown in Figure 4.11B in which the time course of the 53 pS channel openings is compared with that of 31 pS conductance state channel (Figure 4.11C).

In order to characterize burst properties of the 53 pS glycine-gated channel, recordings were reanalyzed ignoring closed time intervals shorter than the double of the faster close time constant. In the presence of 30 μM glycine the burst duration histogram could be fitted with the sum of two exponential curves having the time constants of 0.6 and 410 ms. Similarly values of burst time constants were observed with glycine 300 μM (0.7 and 420 ms for the τb_1 and τb_2 respectively). As the burst time constants also the relative weights, or exponential areas, were not significantly ($p > 0.5$) different in the two experimental conditions.

time constants (ms) areas (%)	30μM glycine	300μM glycine
τo_1	0.94 ± 0.4 (4)	1.6 ± 0.4 (6)
ao_1	0.43 ± 0.09	0.44 ± 0.08
τo_2	140 ± 10 (4)	160 ± 20 (6)
ao_2	0.57 ± 0.09	0.56 ± 0.08
τc_1	12 ± 2.4 (4)	4.7 ± 0.4 (7)
ac_1	0.83 ± 0.03	0.60 ± 0.07
τc_2	2700 ± 910 (4)	1790 ± 590 (7)
ac_2	0.17 ± 0.03	0.40 ± 0.07
τb_1	0.63 ± 0.01 (3)	0.73 ± 0.15 (6)
ab_1	0.62 ± 0.02	0.67 ± 0.05
τb_2	410 ± 50 (3)	420 ± 140 (6)
ab_2	0.38 ± 0.02	0.33 ± 0.05

Table 2. Open (τo_1, τo_2), closed (τc_1, τc_2) and burst (τb_1, τb_2) time constants of 53 pS single channel conductance state activated by glycine (30 and 300 μM) at a holding potential of -40 mV. The corresponding relative areas (ao_x, ac_x, ab_x) of exponential components fitted to histograms, as shown in Figure 4.13A, are normalized to 1. In parenthesis the number of observations.

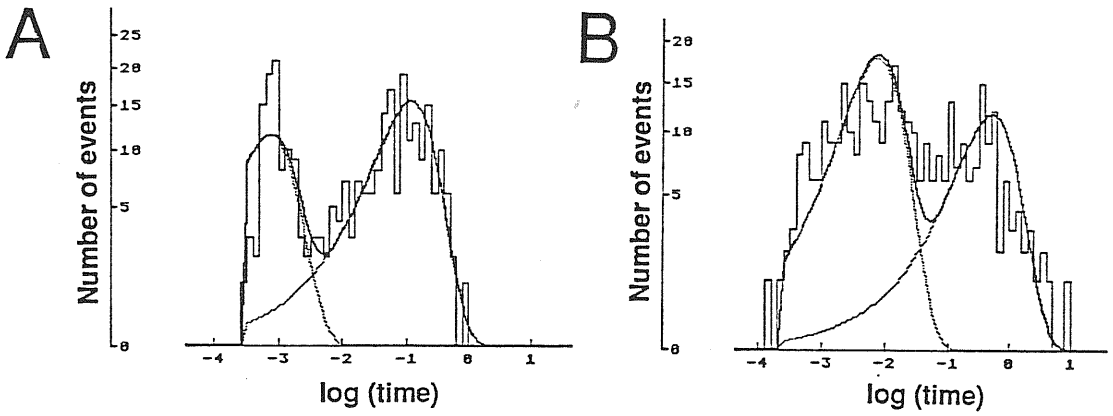

Figure 4.13 Open and closed time histograms activated by glycine (100 μM). The mean open (A) and shut times (B) were fitted with exponential function according to Sigworth and Sine (1987). τo_1 = 0.8 ms and τo_2 = 121 ms. B. τc_1 = 8.1 ms and τc_2 = 530 ms. A and B are from the same experiment.

4.3 Expression of glycine and GABA receptors is developmentally regulated

The expression of glycine and GABA receptors during days in culture in cerebellar granule cells was quantified by calculating the current densities by dividing the total $GABA_A$ or glycine currents evoked by 300 μM of GABA or glycine, by the membrane capacitance, obtained from the compensation of the capacitance transient. Striking differences between $GABA_A$ and glycine activated currents were found during days in culture. All cells tested between 2 and 15 DIC responded to GABA, whereas only 50% responded to glycine (Figure 4.14 inset). Moreover, in contrast to GABA, glycine-evoked current were maximally expressed between the 4th and the 7th DIC. The density of glycine induced currents varied significantly ($p<0.02$) between 4-7 and 8-14 DIC (from 28.3 ± 4.3 pA/pF, n=51 to 11.5 ± 2.1 pA/pF, n=18). In contrast, the density of GABA-evoked currents calculated on the same cells that responded to glycine were not significantly ($p>0.5$) different between 4-7 and 8-14 DIC (346.4 ± 27.7 pA/pF and 348.5 ± 32.3 pA/pF, respectively).

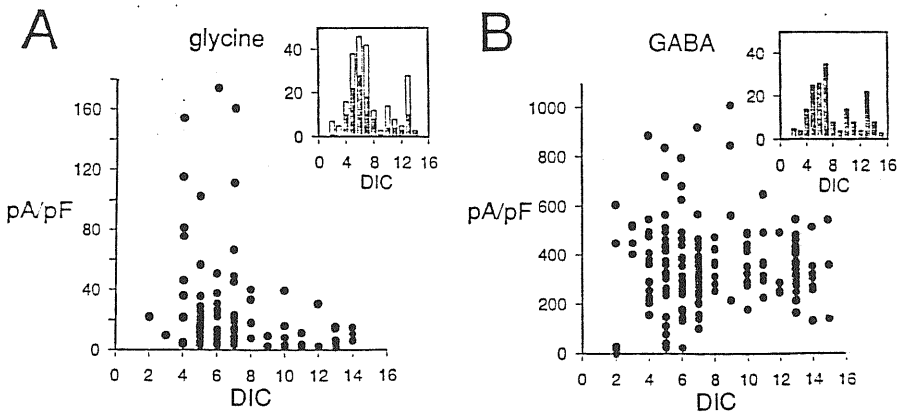

Figure 4.14 Changes in glycine and GABA currents during days in culture. A. Current density (pA/pF) induced by glycine (300 μM) is plotted against days in culture (DIC). Notice that the maximal expression density occurred between 4 and 7 DIC. The graph in the inset represents the number of cells tested (ordinate) versus DIC (abscissa). Only 50% of the cells tested responded to glycine (closed bars). The plot in B. represents the current density (pA/pF) produced by GABA (300 μM) against DIC. The inset represents the number of cell tested versus DIC. Notice that all cells tested responded to GABA.

4.4 Modulation of spontaneous GABAergic synaptic currents by glycine

In our culture conditions (low potassium medium), granule cells exhibit spontaneous synaptic currents mediated by GABA which probably is released from undifferentiated GABAergic interneurons (Virginio et al, 1995). As already mentioned in the introduction in the adult cerebellum most Golgi cell terminals exhibit both GABA- and glycine-like immunoreactivity (Ottersen 1988). Moreover these cells may release both GABA and glycine (Morales and Tapia, 1987). However, in our cultures, the application of 1 μM strychnine failed to induce any change in amplitude or frequency of spontaneous events (n=5). This suggest that endogenous glycine was not released in our culture conditions.

May GlyRs, in these undifferentiated cells have a role in the modulation of GABAergic spontaneous events? To ask this question the following experiments were undertaken to see whether glycine can modulate spontaneous GABA-mediated synaptic currents.

Bath application of glycine (300 μM) produced an inward current of 24.6 ± 17.8 pA and an increase in the baseline noise (n=4). In three cells glycine induced a marked reduction in the frequency of spontaneous GABAergic currents (from 2.3 ± 0.09 to 0.54 ± 0.05 Hz, Figure 4.15A). These values were significantly ($p<0.01$) different. The decrease in frequency of spontaneous synaptic currents was not associated with any significant ($p>0.1$) change in the amplitude of synaptic events (the mean amplitude ratio -control over glycine- was 1.14 ± 0.07) and was rapidly reversed upon wash out of glycine. In one case, glycine produced a three fold increase in frequency of spontaneous GABA-mediated events (from 1.1 to 3.2 Hz, Figure

4.15B). The effects of glycine persisted in the presence of kynurenic acid (1 mM) but were abolished by TTX (1 μM).

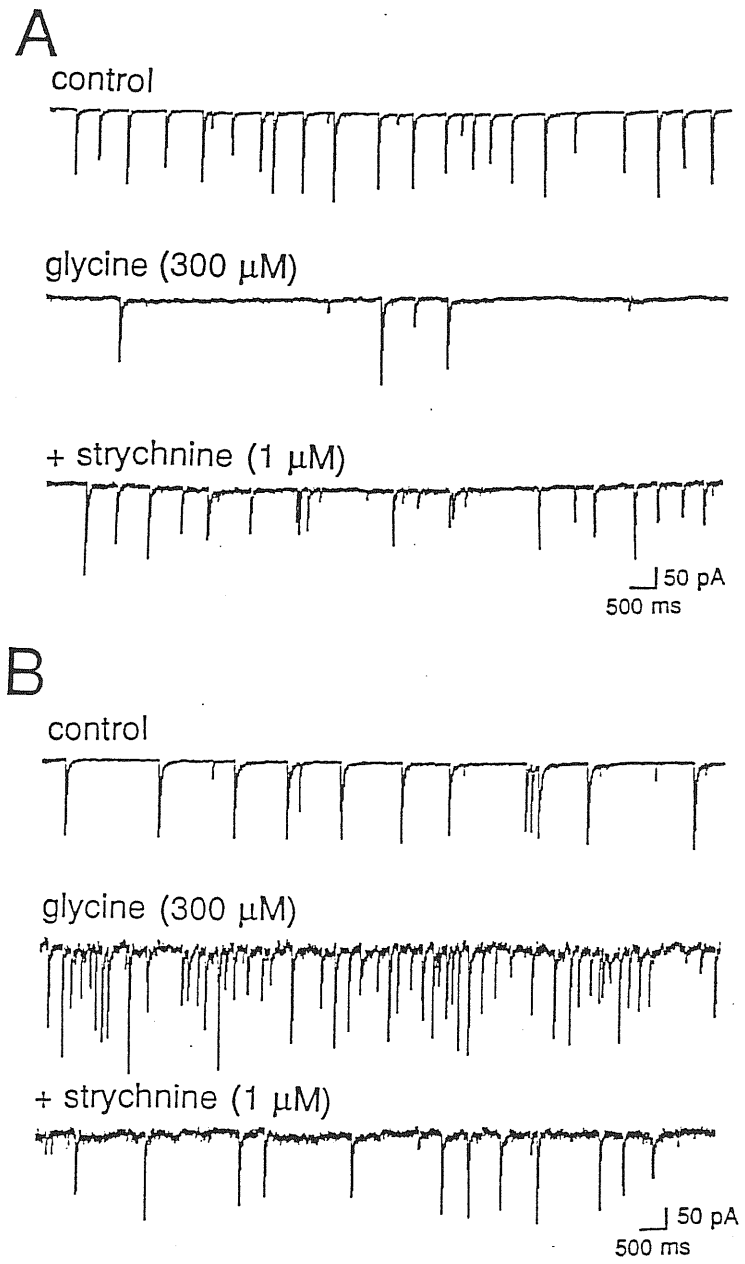

Figure 4.15 Modulatory effects of glycine on spontaneous GABAergic currents. A. Spontaneous currents recorded in the presence of kynurenic acid (1 mM) from a granule cell (7 DIC) held at -60 mV. Application of glycine produced a small inward current (24.6 ± 17.8pA), an increase in the baseline noise and a decrease in the frequency of spontaneous events. This effect was reversed by strychnine (1 μM). B. In another cell (7 DIC), glycine, applied in the presence of kynurenic acid (1 mM) produced a striking increase in frequency of spontaneous events. Also this effect was associated with an increase in the baseline noise and was partially reversed by strychnine.

Chapter 5

Discussion

5.1 Glycine activated whole cell current

The present experiments show that cerebellar granule cells in culture bear functional strychnine-sensitive glycine receptors similar in many aspects to those found in granule cells in thin cerebellar slices (Kaneda et al, 1995) and in other brain structures (Bormann et al, 1987; Ito and Cherubini, 1991; Fatima-Shad and Barry, 1992; Lewis and Faber, 1993). Evidence in favour of the existence of GlyRs in the cerebellar cortex is provided by *in situ* hybridization studies which have demonstrated the presence of GlyR subunits mRNA mainly in the first two weeks of postnatal life (Malosio et al 1991b).

Glycine gated channels were chloride permeable as suggested by the shift in E_{gly} towards more positive voltages in the presence of decreasing concentrations of $[Cl^-]_o$ in the same way as predicted from the Nernst equation. In contrast to other neuronal preparations (Bormann et al, 1987) which show a marked outward rectification, glycine currents present in cultured cerebellar granule cells were voltage independent, at least in the potential range between -40 mV and 40 mV. In this respect they behaved as glycine responses in neonatal hippocampal and medulla oblongata neurons (Krishtal et al, 1988; Ito and Cherubini, 1991).

With higher agonist concentration a slow desensitizing component of glycine-evoked currents has been observed. In comparison to GABA, the desensitization kinetic of glycine currents was slower (Kilic et al, 1993) and the recovery from desensitization was faster (τ_r was 36 and 5 s for GABA and glycine, respectively, Kilic et al, 1993).

Thus, the slow desensitization kinetic and the fast recovery from desensitization would contribute to prolong the action of glycine. The activation of chloride conductance by glycine was competitively and reversibly antagonized by the convulsant alkaloid strychnine, considered the most potent glycine antagonist (Curtis et al, 1968). The effect of strychnine was selective for glycine, since this substance did not modify the response to GABA; on the other hand the selective $GABA_A$-receptor competitive antagonist bicuculline was ineffective on glycine evoked currents, suggesting that glycine was acting *via* a receptor distinct from the $GABA_A$ one. Glycine evoked currents were also reversibly blocked by picrotoxin, thought to bind within the pore of chloride channel and routinely used to block GABA responses (Olsen, 1982). This observation may favour the hypothesis that GABA and glycine responses, although mediated through two distinct receptor types may activate channels having similar properties. However, no occlusion or cross desensitization was found with combined application of GABA and glycine suggesting that these amino acids act on receptors coupled to different chloride channels.

The finding that zinc potentiates glycine responses is also of interest in view of the modulatory role of this divalent cation in synaptic transmission (Smart et al, 1994). Zinc has been shown to depress GABA responses in a non competitive way in the same cultured cell preparation (Kilic et al, 1993). Recently it has been found that in chick ciliary ganglion neurons, glycine induced currents were slightly enhanced by low concentrations of zinc (2-10 μM), whereas at higher concentrations (> 100 μM), zinc substantially inhibited these responses (Zhang and Berg, 1995). A biphasic modulation of glycine currents by zinc was also described in cultured spinal neurons and in oocytes expressing recombinant homo (α_1, α_2) and hetero-oligomeric (α_1/β)

human glycine receptors (Laube et al, 1995). The positive modulation by zinc, obtained when it was applied extracellularly at concentrations of 0.5-10 μM, was abolished in chimeric constructs in which one segment of the α_1 subunit was replaced by the homologous β-cDNA sequence. In these chimeras the negative modulation of glycine responses at higher zinc concentrations was conserved. The positive modulation of glycine response by zinc found in the present experiments allow to exclude the involvment of glycine channels containing exclusively α_1, α_2 subunit or a combination of α_1/β.

5.2 Glycine evoked single channel events

The single-channel study confirmed the existence of distinct class of receptors for GABA and glycine. In fact the single channel conductances found in the present experiments for glycine were clearly different from those activated by GABA in the same preparation (Kilic et al, 1993; Martina, personal communication). The three different conductance states for glycine were in the same range of those found in other neuronal preparations (Bormann et al, 1987; Twyman and MacDonald, 1991; Takahashi and Momiyama, 1991;Takahashi et al, 1992) or in granule cells from thin cerebellar slices (Kaneda et al, 1995). The small difference between the conductance values observed in cerebellar granule cells in slices or in culture may be ascribed to the fact that in the former preparation single channel events were recorded and measured in the whole cell configuration. It is interesting to note that the value of the larger conductance channel found in cerebellar granule cells in culture (84 pS) is similar to that observed in rat spinal cord neurons from neonatal animals (79 pS, Takahashi and Momiyama, 1991) that disappears later in development (Takahashi et al, 1992). Also in oocytes expressing different glycine

receptor subunits combinations from three to six different conductance states have been observed (Bormann et al, 1993). The coexpression of the β with the α_2 subunit induces channels having conductance states of 36, 54 and 80 pS, values very close to those found in the present experiments.

As revealed by kinetic analysis, the 53 pS conductance channel yielded two open, two close and two burst time constants indicating that this channel can exist in several open or close states. The values of open time constants were similar to those reported for glycine evoked single channel currents in spinal cord neurons or in *Xenopus* oocytes expressing α_2 homomeric receptor channels (Takahashi et al, 1992). The similar values found for the fast burst and fast open time constant indicate that they refer to the same event: the brief opening.

Glycine concentration did not affect the mean open, slow close or burst time constants but only reduced the fast close one. The latter correspond to the closures within a burst. These findings suggest that the increase of glycine concentration enhances the open channel probability.

5.3 Molecular model

Glycine receptor is thought to be a pentameric membrane protein composed of 3 α and 2 β subunits (Betz, 1992). Pharmacological, biochemical and cDNA sequence data have revealed marked differences in the regional distribution and developmental expression of glycine receptors (Malosio et al, 1991). A neonatal isoform, characterized by low strychnine binding affinity and containing α_2 subunits of 49 kDa prevails in the spinal cord of neonatal rats (Becker et al, 1988). This developmentally regulated subunit is also expressed in the cerebral cortex and in the hippocampus (Malosio et al, 1991; Akagi et al, 1991; Becker et al, 1993). Also

cerebellar granule cells in culture are likely to express the α_2 glycine receptor subunit as suggested by Wahl et al (1994) on the basis of the relative sensitivity to β-alanine and taurine. The co-expression of the α_2 and β subunits results in hetero-oligomeric channels that are less sensitive to picrotoxinin, the toxic component of picrotoxin: the IC_{50} value for picrotoxinin in homo-oligomeric channels was in the range of 5-9 μM while it was > 1mM for α_1/β and α_3/β hetero-oligomers and 300 μM for α_2/β hetero-oligomer (Pribilla et al, 1992). Our observations that glycinergic currents were moderately sensitive to picrotoxin (EC_{50} = 172 μM) are compatible with the presence of both homo-oligomeric (α_2) and/or hetero-oligomeric (α_2/β) channnels. In this respect our findings differ from those of Kaneda et al (1995) in which the responses to glycine were insensitive to 100 μM of picrotoxin (in our case this concentration caused a 35% block).

Furthermore the co-expression of the β with the α_2 subunit induces channels with conductance states of 36, 54 and 80 pS (Bormann et al, 1993). On the other hand expression of the α_2 subunit alone induces the expression of channels having conductances of 36, 48, 66, 91 and 111 pS (Bormann et al, 1993). It is therefore possible that the native glycine receptors present in cerebellar granule cells in culture result from the assembling of the α_2 and β subunits. The β subunit infact is widely expressed either in neonatal or in adult brain (Malosio et al, 1991). Furthermore the open time constants obtained from the analysis of 53 pS conductance channel confirm the presence of the α_2-subunit in our preparation (Takahashi et al, 1992).

It is interesting to note that, in comparison to GABA, glycine current density changed drastically with DIC, the maximal expression being between the 4th and the 7th DIC. This probably reflects changes in synthesis of channel proteins and not loss of a

neuronal population as indicated by the fact that the same cells were still able to respond to GABA. It appears, therefore, that the expression of glycine receptors in the cerebellum is developmentally regulated as shown by *in situ* hybridization studies (Malosio et al, 1991).

5.4 Physiological role of glycine receptors

In the adult rat cerebellum, granule cells are inhibited by Golgi interneurons, whose terminals show strong glycine-like immunoreactivity (Ottersen et al, 1988). Ottersen et al (1990) have also demonstrated that Golgi terminals co-release glycine and GABA. In cultured cerebellar granule cells grown in a low potassium medium, although GABA-mediated synaptic currents have been recently described (Virginio et al, 1995), no glycinergic events have been detected. Therefore, even if GlyRs are present in our cultured neurons, they are not activated synaptically by the release of endogenous glycine, as shown by the lack of effect of strychnine on spontaneous synaptic currents. Activation of GlyR by exogenously applied glycine caused a strong inhibition of GABA release, measured by the reduction in the frequency of the spontaneous GABA-mediated synaptic events. In keeping with these results are the observations of Wahl et al (1994) that showed a strong depression of the K^+-evoked release of D-[^{3}H]-aspartate following activation of glycine receptors. The excitatory effect of glycine on GABA release found in one experiment and also described by Kaneda et al. (1995) in granule cells from thin cerebellar slices, is compatible with a depolarizing action of this amino acid during development (Ito and Cherubini, 1991; Cherubini et al, 1991). A different degree of maturity of cultured GABAergic neurons may be responsible for the shift in the Cl^- equilibrium potential and therefore for the excitatory or inhibitory effects of glycine on spontaneous GABAergic currents. In the

present study, 50% of tested neurons were responsive to glycine. This heterogeneity in glycine sensitive cells may reflect again different developmental states of individual neurons.

In conclusion the present data indicate that cultured granule cells express the gene for the glycine receptor and this expression is developmentally regulated. A developmental regulation of GlyR expression has been also demonstrated in the cerebellum in vivo (Malosio et al 1991). Therefore cerebellar granule cells in culture could be a good model to study the possible role of GlyRs in the development of cerebellum and the factors influencing their expression.

Refences

Akagi H and Miledi R (1988) Heterogeneity of glycine receptors and their messanger RNAs in rat brain and spinal cord. *Science* 242:270-273.

Akagi H, Patton DE and Miledi R (1989) Discrimination of heterogenous mRNAs encoding strychnine-sensitive glycine recepors in *Xenopus* oocytes by antisense oligonucleotides. *Proc Natl Acad Sci USA* 86:8103-8107.

Akagi H, Hirai K and Hishinuma F (1991) Cloning of a glycine receptor subtype expressed in rat brain and spinal cord during a specific period of neuronal development. *FEBS Lett* 281:160-166.

Akaike N, Shirasaki T and Yakushiji T (1991) Quinolines and Fenbuten interact with $GABA_A$ receptor in dissociated hippocampal cells of rat. *J Neurophysiol* 6:1400-1409.

Altschuler RA, Betz H, Parakkal MH, Reeks KA and Wenthold RJ (1986) Identification of glycinergic synapses in the cochlear nucleus through immunocytochemical localization of the postsynaptic receptor. *Brain Res* 369:316-320.

Balázs R, Jørgensen O S and Hack N (1988) N-Methyl-D-aspartate receptor promotes the survival of cerebellar ranule cells in culture. *Neuroscience* 27:437-451.

Barish ME (1983) A transient calcium-dependent chloride current in the immature *Xenopus* oocyte. *J Physiol (Lond)* 342:309-325.

Barnard EA, Darlison MG and Seeburg PH (1987) Molecular biology of the $GABA_A$ receptor: the receptor/channel superfamily. *Trends in Neurosci* 10:502-509.

Barnard EA (1992) Subunits of $GABA_A$, glycine, and glutamate receptors. in *Receptor subunit and complexes*, Burger A & Barnard EA (eds), Cambridge University Press pp163-187.

Becker C-M, Hoch W and Betz H (1988) Glycine receptor heterogeneity in rat spinal cord during postnatal development. *EMBO J* 7:3717-3726.

Becker C-M, Hoch W and Betz H (1989) Sensitive immunoassay shows selective association of peripheral and integral membrane proteins of the inhibitory glycine receptors complex.*J Neurochem* 53:125-131.

Becker C-M (1992) Convulsant acting at the inhibitory glycine receptor. In *Handbook of experimental Pharmacology* . 102 *Selective Neurotoxicity* (ed. H. Herken and F. Hucho). Berlin, Heidelberg: Springer-Verlag.

Becker C-M, Betz H and Schröder H (1993) Expression of inhibitory glycine receptors in post natal rat cerebral cortex. *Brain Res* 606:220-226.

Betz H (1987) Biology and structure of the mammalian glycine receptors. *TINS* 10:113-117.

Betz H (1990) Ligand-gated ion channels in the brain: the amino acid receptor superfamily. *Neuron* 5:383-392.

Betz H (1991) Glycine receptors: heterogeneous and widespread in the mammalian brain. *TINS* 14:458-461.

Betz H (1992) Structure and function of inhibitory glycine receptors. *Quart Rev Bioph* 25:381-394.

Bisti S, Iosif G, Marchesi GF and Strata P (1971) Pharmacological properties of inhibitions in he cerebellar cortex. *Exp Brain Res* 14:24-37.

Bormann J, Hamill OP and Sakmann B (1987) Mechanism of anion permeation through channels gated by glycine and γ-aminobutyric acid in mouse cultured spinal neurones. *J Phisiol* 385:243-286.

Bormann J, Rundström N, Betz H and Langosch D (1993) Residues within transmembrane segment M2 determine chloride conductance of glycine receptor homo- and hetero-oligomers. *EMBO J* 12:3729-3737.

Brake AJ, Wagenbach MJ and Julius D (1994) New structural motif for ligand-gated ion channels defined by an ionotropic ATP receptor. *Nature* 371:519-523.

Cherubini E, Gaiarsa JL and Ben-Ari Y (1991) GABA: an excitatory transmitter in early postnatal life. *TINS* 14:515-519.

Cull-Candy SG, Miledi R and Parker I (1981) Single glutamate activated channel recorded from locust muscle fibers with perfused patch electrodes. *J Physiol* 321:195-210.

Cull-Candy SG, and Usowicz MM (1989) Whole-cell current noise produced by excitatory and inhibitory amino acids in large cerebellar neurons of the rat. *J Physiol* 415:533-553.

Curtis DR, Hosli L, Johnston GAR and Johnston IH (1968) The hyperpolarization of spinal motoneurons by glycine and related amino acids. *Exp Brain Res* 5:235-256.

Curtis DR and Johnston GAR (1974) Amio acid transmitters in the mammalian central nervous system. *Ergebn Physiol* 69:97-188.

Dionne VE and dLiebowitz MD (1982) Acetylcholine receptor kinetics: a description from single channel currents at snake neuromuscolar junctions. *Bioph J* 39:253-261.

Dvergsten CL, Fosmire CJ, Ollerich DA and Sandstead HH (1983) Alterations of the postnatal development of the cerebellar cortex due to zinc deficiency. I. Impaired aquisition of granule cells. *Brain Res* 271:217-226.

Faber H, Braun K, Zuschratter W and Scheich H (1989) System-specific distribution of zinc in the chick brain. *Cell Tissue Res* 258:247-257.

Fatima-Shad K and Barry PH (1992) A patch-clamp study of GABA and strychnine-sensitive glycine-activated currents in postnatal tissue-cultured hippocampal neurons. *Proc R Soc Lond [Biol]* 250:99-105.

Frederickson CJ (1989) Neurobiology of zinc and zinc-containing neurons. *Int Rev Neurobiol* 31:145-238.

Frostholm A and Rotter A (1985) Glycine receptor distribution in mouse CNS: autoradiographic localization of [^{3}H]strychnine binding sites. *Brain Res Bull* 15:473-486.

Frost White W, O'Gorman S and Roe AW (1990) Three-dimensional autoradiographic localization of quench-corrected glycine receptor specific activity in the mouse brain using [^{3}H]strychnine as the ligand. *J Neurosci* 10:795-813.

Gallo V, Kingsbury A, Balázs R and Jørgensen OS (1987) The role of depolarization in the survival and differentiation of cerebellar granule cells in culture. *J Neurosci* 7:2203-213.

Gao W-Q, Heintz N and Hatten M (1991) Cerebellar granule cell neurogenesis is regulated by cell-cell interactions in vitro. *Neuron* 6:705-715.

Garcia-Calvo M, Ruiz-Gómez A, Vazquez J, Morato E, Valdivieso F and Major F Jr (1989) Functional reconstitution of the glycine receptor. *Biochemistry* 28:6405-6409.

Graham D, Pfeiffer F and Betz H (1983) Photoaffinity-labeling of the glycine receptor of rat spinal cord. *Eur J Biochem* 131:519-525.

Grenningloh G, Gundelfinger ED, Schmitt B, Betz H, Darlison MG, Barnard EA, Schofield PR and Seeburg PH (1987a Glycine vs GABA receptors. *Nature* 330:25-26.

Grenningloh G, Rienitz A, Schmitt B, Methfessel C, Zensen M, Beyreuther K, Gundelfinger ED and Betz H (1987b)The strychnine binding subunit of the glycine receptor shows homology with nicotinic acetylcholine receptors. *Nature* 328:215-220.

Grenningloh G, Pribilla I, Prior P, Multhaup G, Beyreuther K, Taleb O and Betz H (1990a) Cloning and expression of the 58 kd β subunit of the inhibitory glycine receptor. *Neuron* 4:963-970.

Grenningloh G, Schmieden V, Schofield PR, Seeburg PH, Siddiqque T, Mohandas TK, Becker CM and Betz H (1990b) Alpha subunit variants of the human glycine receptor: prymary structures, functional expression and chromosomal localization of the corresponding genes. *EMBO J* 9:771-776.

Hamill OP, Marty A, Neher E, Sakmann B and Sigworth FJ (1981) Improved patch-clamp techniques for high resolution current recording from cells and cell free membrane patches. *Pflügers Arch* 391:85-100.

Hamill OP, Bormann J and Sakmann B (1983) Activation of multiple conductance state chloride channels in spinal neurons by glycine and GABA. *Nature* 305:85-100.

Hille B (1992) *Ionic channels of exitable membranes.* (2nd editioon), Sinauer Associated Inc. (eds), Sunderland, Massachusetts.

Horikoshi T, Asanuma A, Yanagisawa K and Goto S (1988) Taurine modulates glycine response in Xenopus oocytes injected with messanger RNA from mouse brain. *Mol Brain Res* 4:243-246.

Huck S and Lux HD (1987) Patch-clamp study of ion channels activated by GABA and glycine in cultured cerebellar neurons of the mouse. *Neurosci Lett* 79:103-107.

Imoto K, Busch C, Sakmann B, Mishina M, Konno T, Nakai J, Bujo H, Mori Y, Fukuda K and Numa S (1988) Rings of negtively charged amino acids determine the acetylcholine receptor channel conductance. *Nature* 355:645-648.

Irving AJ, Schofield JG and Collingridge GL (1992) The effect of $[K^+]$ during culture on the appearance of spontaneous $[Ca^{2+}]$ oscillations in rat cerebellar granule cells. *Soc Neurosci Abs* 18:46.

Ito S and Cherubini E (1991) Strychnine-sensitive glycine responses of neonatal rat hippocapal neurones. *J Physiol (Lond)* 440:67-83.

Kandel ER, Schwartz JH and Jessell TM (1991) *Principles of neural science.* (3rd edition), Elsevier Science Publishing Inc., New York.

Kaneda M, Farrant M and Cull-Candy SG (1995) Whole-cell and single-channel currents activated by GABA and glycine in granule cells of the rat cerebellum. *J Phisiol (Lond)* 485:419-435.

Kelly JS and Krnjevic K (1968) Effect of the gamma-aminobutyric acid and glycine on cortic l neurons. *Nature* 219:1380-1381.

Kilic G, Moran O and Cherubini E (1991) N-Methyl-D-aspartate receptor-mediated spontaneous activity in cerebellar granule cells in culture. *Neurosci Lett* 130:263-266.

Kilic G, Moran O and Cherubini E (1993) Currents activated by GABA and their modulation by Zn^{2+} in cerebellar granule cells in culture. *Europ J Neurosci* 5:65-72.

Kirsch J, Langosch D, Prior P, Littauer UZ, Schmitt B and Betz H (1991) The 93 kDa glycine receptor-associated protein binds to tubulin. *J Biol Chem* 266:22242-22245.

Kirsch J, Malosio M-L, Wolters I and Betz H (1993a) Distribution of gephirin transcripts in the adult and developing rat brain. *Eur J Neurosci* 5:1109-1117.

Kirsch J, Wolters I, Triller A and Betz H (1993b)Gephyrin antisense oligonucleotides prevent clustering in spinal neurones. *Nature* 366:745-748.

Krishtal OA, Osipchuk YV and Vrublevsky SV (1988) Properties of glycine-activated conductances in rat brain neurons. *Neurosci Lett* 84:271-276.

Krupp J and Feltz P (1993) Synaptic- and agonist-induced chloride currents in neonatal rat sympathetic preganglionic neurones *in vitro*. *J Physiol* 471:729-748.

Kuhar SG, Feng L, Vidan S, Ross ME, Hatten ME and Heinz N (1993) Changing patterns of gene expression define four stages of cerebellar granule neuron differentiation. *Development* 117: 97-104.

Kuhse J, Schmieden V and Betz H (1990a) A single amino acid exchange alters the pharmacology of neonatal rat glycine receptor subunit. *Neuron* 5:867-873.

Kuhse J, Schmieden V and Betz H (1990b) Identification and functional expression of a novel ligand binding subunit of the inhibitory glycine receptor. *J Biol Chem* 265:22317-22320.

Kuhse J, Kuriatov A, Malosio ML, Schmieden V and Betz H (1991) Alternative splicing generates two isoforms of the alpha 2 subunit of the inhibitory glycine receptor. *FEBS Lett* 283:73-77.

Kyte J and Dolittle RF (1982) A method for displaying the hydrophobic character of a protein. *J Mol Biol* 157:105-132.

Hoch W, Betz H and Becker C-M (1989) Primary cultures of mouse spinal cord express the neonatal isoform of the inhibiory glycine receptor. *Neuron* 3:339-348.

Langosch D, Thomas L and Betz H (1988) Conserved quaternary structure of ligand-gated ion channels: the postsynaptic glycine receptor is a pentamer. *Proc Natl Acad Sci USA* 85:7394-7398.

Langosch D, Becker CM and Betz H (1990) The inhibitory glycine receptor: a ligand-gated chloride channel of the central nervous system. *Eur J Biochem* 194:1-8.

Laube B, Kuhse J, Rundström N, Kirsch J, Schmieden V and Betz H (1995) Modulation by zinc ions of native rat and recombinant human inhibitory glycine receptors. *J Physiol [Lond]* 483:613-619.

Legendre P and Korn H (1994) Glycinergic inhibitory synaptic currents and related receptor channels in the zebrafish brain. *Europ J Neurosci* 6:1544-1557.

Levi G, Aloisi F, Ciotti MF and Gallo V (1984) Autoradiographic localization and depolarization-induced release of acidic amino-acids in differentiating cerebellar granule cell cultures. *Brain Res* 290:77-86.

Lewis CA and Faber DS (1993) GABA responses and their partial occlusion by glycine in cultured rat medullary neurons. *Neurosci* 52:83-96.

Malosio ML, Grenningloh G, Kuhse J, Schmieden V, Schmitt B, Prior P and Betz H (1991) Alternative splicing generates two variants of the alpha 1 subunit of the inhibitory glycine receptor. *J Biol Chem* 4:2048-2053.

Malosio ML, Marquèze-Pouey B, Kuhse J and Betz H (1991) Widespread expression of glycine receptor subunit mRNAs in the adult and developing rat brain. *EMBO J* 10:2401-2409.

Matzenbach B, Maulet Y, Sefton L, Courtier B, Avner P, Guenet JL and Betz H (1994) Structural analysis of mouse glycine receptor alpha subunit genes. Identification and chromosomal localization of a novel variant. *J Biol Chem* 269:2607-2612.

Miledi R, Parker I and Sumikawa K (1989) Transplanting receptors from brains into oocytes. *Fidia Res Found Neurosci Award Lect* 3:57-90.

Mishina M, Tobimatsu T, Imoto K, Tanaka K, Fujita Y, Fukuda K, Kurasaki M, Takahashi H, Morimoto Y, Hirose T, Inayama S, Takahashi T, Kuno M and Numa S (1985) Localization of functional regions of acetylcholine receptor alpha-subunit by site-directed mutagenesis. *Nature* 313:364-369.

Morales E and Tapia R (1987) Neurotransmitters of the cerebellar glomeruli: uptake and release of labelled gamma-amiinobutyric acid, glycine, serotonin and choline in a purified glomerolus fraction and in granular layer slices. *Brain Res* 420:11-21.

Morales A, Nguyen Q-T and Miledi R (1994) Electrophysiological properties of newborn and adult rat spinal cord glycine receptors expressed in *Xenopus* oocytes. *Proc Natl Acad Sci USA* 91:3097-3101.

Naas E, Zilles K, Gnahn H, Betz H, Becker C-M and Schröder H (1991) Glycine receptor immunoreactivity in rat and human cerebral cortex. *Brain Res* 561:139-146.

Nauma WJH and Feirtag M (1986) *Fundamental neuroanatomy*. W. H. Freeman and Company (eds), New York.

Noda M, Takahashi H, Tanabe T, Toyosato M, Kiyotani S, Furutani Y, Hirose T, Takashima H, Inayama S, Miyata at and Numa S (1983) Structural homology of Torpedo californica acetylcholine receptor subunits. *Nature* 302:528-532.

Neher E and Sakmann B (1976) single-channel currents recorded from membrane of denervated frog muscle fibers. *J Physiol* 277:153-176.

Numa S (1989) A molecular view of neurotransmitter receptors and ionic channels. *Harvey Lect* 83:121-165.

Olsen RW (1982) Drug interaction at the GABA receptor-ionophore complex. *Annual rev Pharmcol Toxycol* 22:245-277.

Ottersen OP, Storm-Mathisen J and Somogyi P (1988) Colocalization of glycine-like and GABA-like immunoreactivities in Golgi cell terminals in the rat cerebellum: a postembedding liight and electron micoscopy study. *Brain Res* 450:342-353.

Ottersen OP, Storm-Mathisen J and Laake J (1990) Cellular and subcellular localization of glycine studied b quanntitative electron microscopic immunocytochemitry. in *Glycine Neurotransmission* (Ottersen OP, Storm-Mathisen J eds) p303. Wiley, Chichester.

Perez-Clausell J, Frederickson CJ and Danscher G (1989) Amygdaloid efferents trhough the stria terminalis in the rat give origin to zinc-contaiing boutons. *J comp Neurol* 290:201-212.

Pfeiffer F, Graham D ad Betz H (1982) Purification by affinity cromatografy of the glycine receptor of the rat spinal cord. *J Biol Chem* 257:9389-9393.

Pfeiffer F, Simler R, Grenningloh G and Betz H (1984) Monoclonal antibodies and peptide mapping reveal structural similarities between the

subunits of the glycine receptor of rat spinal cord. *Proc Natl Acad Sci USA* 81:7224-7227.

Pribilla I, Tamaki T, Langosch D, Bormann J and Betz H (1992) The atypical M2 segment of the β subunit confers picrotoxinin resistance to inhibitory glycine receptor channels. *EMBO J* 11:4305-4311.

Probst A, Cortes R and Palacios JM (1986) The distribution of glycine receptors in the ehuman brain. A light microscopic autoradiographic study using [^{3}H]strychnine. *Neurosci* 17:11-35.

Rakic P (1971) Neuron-glia relationship during granule cell migration in developing cerebellar cortex. A Golgi and electron microscopic study in Macacus rhesus. *J Comp. Neurol.* 141:283-312.

Randal AD, Deisseroth K and Tsien RW (1993) Excitatory and inhibitory synaptic connectivity between cultured rat cerebellar granule cells. *J Physiol* 473:153P.

Ruiz-Gómez A, Morato E, Garcia-Calvo M, Valdivieso F and Major F Jr (1990) Localization of the strychnine binding site on the 48-kilodalton subunit of the glycine receptor. *Biochemistry* 29:7033-7040.

Ruiz-Gómez A, Vaello ML and Valdivieso F and Mayor F Jr (1991) Phosphorilation of the 48-kDa subunit of the glycine receptor by protein kinase C. *J Biol Chem* 266:559-566.

Sakmann B, Hamill OP and Bormann J (1983) Patch-clamp measurements of elementary chloride currents activated by the putative inhibitory transmitters GABA and glycine in mammalian spinal neurons. *J Neural Transmission Supplementum* 1:83-95.

Schmieden V, Grenningloh G, Schofield PR and Betz H (1989) Functional expression in Xenopus oocytes of the strychnine binding 48 Kd subunit of the glycine receptor. *EMBO J* 8:695-700.

Schmieden V, Kuhse J and Betz H (1992) Agonist pharmacology of neonatal and adult glycine receptor α subunits: identification of amino acid residues involved in taurine activation. *EMBO J* 11:2025-2032.

Schmieden V, Kuhse J and Betz H (1993) Mutation of glycine receptor subunit creates β-alanine receptor responsive to GABA. *Science* 262:256-258.

Schmitt B, Knaus P, Becker CM and Betz H (1987) The M_r 93 0000 polypeptide of the postsynaptic glycine receptor complex is peripheral membrane protein. *Biocemistry* 26:805-811.

Schofield PR, Darlison M, Fujita N, Burt D, Stephenson F, Rodriguez F, Rhee L, Ramachandran J, Reale V, Glencorse T, Seeburg PH and Barnard EA (1987) Sequence and functional expression of the $GABA_A$ receptor shows a ligand gated receptor superfamily. *Nature* 328:221-227.

Schönrock B and Bormann J (1995) Modulation of hippocampal glycine receptor channels by protein kinase C. *NeuroReport* 6:301-304.

Schröder C, Hoch W, Becker C-M, Grenningloh G and Betz H (1991) Mapping of antigenic epitopes on the alpha 1 subunit of the inhibitory glycine receptor. *Biochem* 30:42-47.

Siebler M, Pekel M, Koller H and Müller HW (1993) Srtychnine-sensitive glycine receptors in cultured primary neurones from rat neocortex. *Develop Brain Res* 73:289-292.

Sigel E and Barnard EA (1984) γ-Aminobutyric acid/benzodiazepine receptor complex from bovine cerebral cortex. *J Biol Chem* 259:7219-7223.

Sigworth FJ (1985) An example of analysis. In *Single-channel recording* edit by Sakmann B and Neher E, Plenum Press. pp 301-322.

Sigworth FJ and Sine SM (1987) Data transformation for the improved display and fitting of single channel dwell time histograms. *Bophys J* 52:1047-1054.

Slomianka L (1992) Neurons of origins of zinc-containing pathways and the distribution of zinc containing boutons in the hippocampal region of the rat. *Neuroscience* 48:325-352.

Smart TG (1992) A novel modulatory binding site for zinc on the $GABA_A$ recepor complex in cultured rat neurones. *J Physiol* 447:587-625.

Smart TG, Xie X and Krishek BJ (1994) Modulation of inhibitory and excitatory amino acid receptor ion channels by zinc. *Progress in Neurobiol* 42:393-441.

Sontheimer H, Becker CM, Pritchett DB, Schofield PR, Grenningloh G, Kettenmann H, Betz H and Seeburg PH (1989) Functional chloride channels by mammalian cell expression of rat glycine receptor subunit. *Neuron* 2:1491-1497.

Stelzer A, Kay AR and Wong RKS (1988) $GABA_A$-receptor function in hippocampal cells is mantained by phosphorilation factors. *Science* 241:339-341.

Surprenatant A, Buell G and North RA (1995) P_{2X} receptors bring new structure to ligand-gated ion channels. *Trends Neurosci* 18: 224-229.

Takahashi T and Momiyama A (1991) Single-channel currents underlying glycinergic inhibitory postsynaptic responses in spinal neurones. *Neuron* 7:965-969.

Takahashi T, Momiyama A, Hirai K, Hishinuma F and Akagi H (1992) Functional correlation of fetal and adult forms of glycine receptors with

developmental changes in inhibitory synaptic receprotr channels. *Neuron* 9:1155-1161.

Thangnipon W, Kingsbury A, Webb M and Balázs R (1983) Observations on rat cerebellar cells in vitro: influence of substratum, potassium concentration and relationship between neurons and astrocytes. *Dev Brain Res* 11:177-189.

Triller A, Cluzeaud F, Pfeiffer F, Betz H and Korn H (1985) Distribution of glycine receptors at central synapses: an immunoelecron microscopy study. *J Cell Biol* 101:683-688.

Triller A, Cluzeaud F and Korn H (1987) Gamma-aminobutyric acid-containing terminals can be apposed to glycine receptors. *J Cell Biol* 104:947-956.

Twyman RE and MacDonald R (1991) Kinetic properties of the glycine receptor main- and sub-conductance states of mouse spinal cord nerones in culture. *J Physiol* 435:303-331.

Unwin N (1993) Neurotansmitter action: opening of ligand-gated ion channels. Cell 72/Neuron 10 (Suppl.):31-41.

Vaello ML, Ruiz-Gómez A and Mayor F (1992) Glycinergic ligands modulate the rate of phosphorylation of the glycine receptor by protein kinase C. *Biochem Biophys Res Commun* 188:813-819.

Vaello ML, Ruiz-Gómez A Lerma J, Mayor F Jr (1994) Modulation of inhibitory glycine receptors by phosphorilation by protein kinase C and cAMP-dependent protein kinase. *J Biol Chem* 269:2002-2008.

Valera S, Hussy N, Evans RJ, Adami N, North RA, Surprenant A and Buell G (1994) A new class of ligand-gated ion channel defined P_{2X} receptor for extracellular ATP. *Nature* 371:516-519.

Vandenerg RJ, French CR, Barry PH, Shine J and Schofield PR (1992) Antagonism of ligand-gated ion channel receptors: two domains of the glycine receptor α subunit form the strychnine-binding site. *Proc Natl Acad Sci USA* 89:1765-1769.

Van den Pol AN and Gorcs T (1988) Glycine and glycine receptor imunoreactivity in brain and spinal cord. *J Neurosci* 8:472-492.

Van der Valk JBF, Resnik A and Balázs R (1991) Membrane depolarization and the expression of glutamete receptors in cerebellar granule cells. *Eur J Pharmacol* 201:247-250.

Virginio C, Martina M and Cherubini E (1995) Spontaneous GABA-mediated synaptic currents in cerebellar granule cells in culture. *Neuro Report* 6:1285-1289.

Wahl P, Elster L and Schousboe A (1994) Identification and function of glycine receptors in cultured cerebellar granule cells. *J Neurochem* 62:2457-2463.

Whiting P, McKernan RM and Iversen LL (1990) Another mechanism for creating diversity in γ-aminobutyrate type A receptors: RNA splicing directs expression of two forms of γ2 subunit, one of which contains a protein kinase C phosphorilation site. *Proc Natl Acad Sci USA* 87:9966-9970.

Wilkin GP, Csillag A, Balázs R, Kingsbury AE, Wilson JE AND Johnson AL (1981) Localization of high affinity [^{3}H]glycine transport sites in the cerebellar cortex. *Brain Res* 216:11-33.

Young AB and Snyder SH (1973) Strychnine binding associated with glycine receptors of the central nervous system. *Proc Natl Acad Sci USA* 70:2832-2836.

Young AB and Snyder SH (1974) Strychnine binding in rat spinal cord membranes associated with the synaptic glycine receptor: cooperativity of tglycine interactions. *Mol Pharmacol* 10:7790-809.

Zarbin MA, Wamsley JK and Kuhar MJ (1981) Glycine receptor light microscopic autoradiographic localization with [^{3}H]strychnine. *J Neurosci* 1:532-547.

Zhang ZW and Berg DK (1995) Patch-clamp analysis of glycine-induced currents in chick ciliaary ganglion neurons. *J Physiol* 487:305-405.